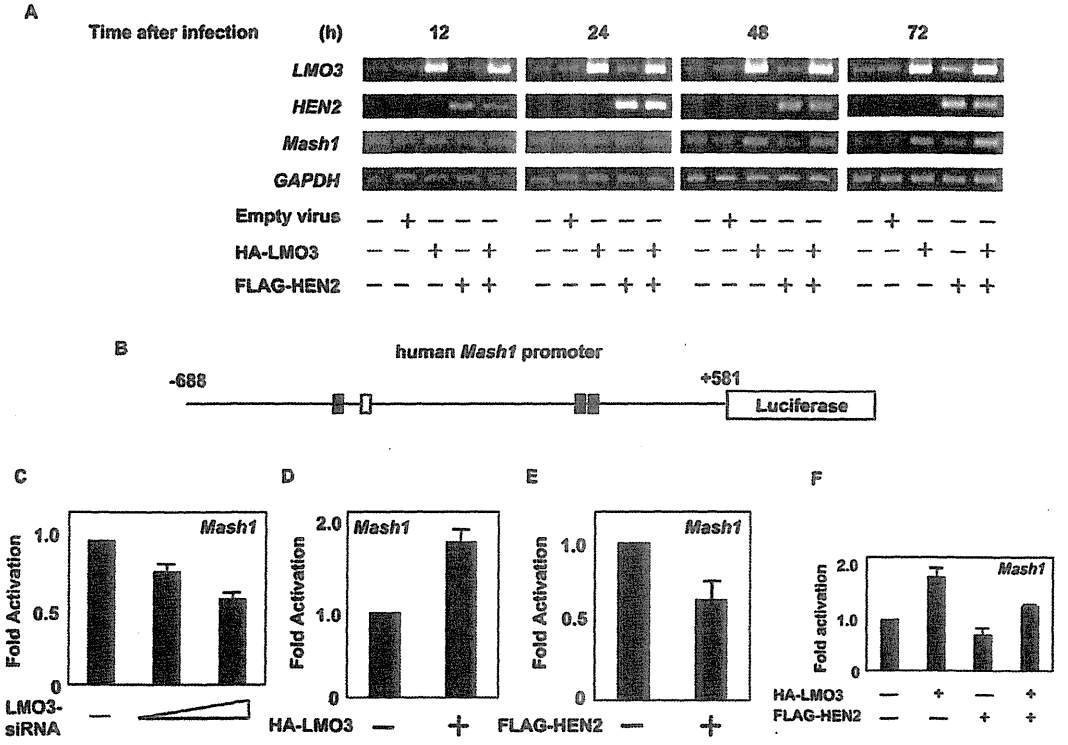

Figure 3. LMO3/HEN2-mediated transcriptional induction of Mash1. (A) RT-PCR. SH-SY5Y cells were infected with empty adenovirus or with the indicated combinations of recombinant adenovirus encoding HA-LMO3 or FLAG-HEN2. At the indicated time points after infection, total RNA was analyzed for expression levels of *LMO3*, *HEN2* and *Mash1* by RT-PCR. *GAPDH* was used as an internal control. (B) Schematic drawing of human *Mash1* promoter. Nucleotide positions were indicated relative to transcriptional initiation site (+1). The putative HES1-binding sites and E-box were depicted by filled and open boxes, respectively. This genomic fragment was subcloned into appropriate restriction sites of pGL3-Basic Vector to give pluc-hMash1. (C) siRNA-mediated knockdown of LMO3 reduces the promoter activity of *Mash1*. SH-SY5Y cells were co-transfected with constant amount of pluc-Mash1 (100 ng) and pRL-CMV (0.2 ng) in the presence or absence of increasing amounts of expression plasmid for siRNA against human LMO3 (100 or 400 ng). Forty-eight hours after transfection, cells were lysed and their luciferase activities were measured. (D) LMO3 transactivates *Mash1* promoter. Mouse neuroblastoma Neuro2a cells (1×10^5 cells/24-well plate) were co-transfected with constant amount of pluc-hMash1 (100 ng) and pRL-CMV (0.2 ng) together with or without expression plasmid for HA-LMO3 (150 ng). Forty-eight hours after transfection, cells were lysed and their luciferase activities were measured. (E) HEN2 inhibits *Mash1* promoter activity. Luciferase activities were measured in Neuro2a cells with or without FLAG-HEN2 (100 ng). (F) LMO3 interferes with negative effect of HEN2 on Mash1 transcription in Neuro2a cells. Luciferase activities were measured in Neuro2a cells transfected with HA-LMO3 (150 ng), FLAG-HEN2 (100 ng) or both of them.
doi:10.1371/journal.pone.0019297.g003

To ask about mechanistic insights into understanding how LMO3 and/or HEN2 could attenuate the inhibitory effects of HES1 on *Mash1* expression, we performed chromatin immunoprecipitation (ChIP) assay. Similar to human *Mash1* promoter, mouse *Mash1* promoter also contains three putative HES1-binding sites and one E-box (Figure 4C). Neuro2a cells were transfected with constant amount of empty plasmid or with expression plasmid for Myc-HES1 together with or without increasing amounts of FLAG-HEN2 expression plasmid. Forty-eight hours after transfection, cross-linked chromatin was prepared and subjected to ChIP assay. As shown in Figure 4D, the anti-Myc tag immunoprecipitates contained genomic fragments including putative HES1-binding sites as well as E-box. The amounts of Myc-HES1 recruited onto HES1-binding sites and E-box significantly decreased in the presence of FLAG-HEN2 in a dose-dependent manner. Additionally, the anti-FLAG immunoprecipitates contained genomic fragments including putative HES1-binding sites and E-box in the absence of exogenous HES1. Co-expression of FLAG-HEN2 and Myc-HES1 inhibited recruitment of FLAG-HEN2 onto putative HES1-binding sites and E-box, however, its inhibition was efficiently abrogated by increasing amounts of FLAG-HEN2. These results suggest that HEN2 might compete with HES1 in binding to putative HES1-binding sites and E-box, and thereby inducing the expression of *Mash1*.

HEN2 Interacts with HES1 in cells

To examine whether HEN2 could interact with HES1 in cells, we performed immunoprecipitation experiments. Cell lysates prepared from Neuro2a cells co-transfected with the indicated combinations of expression plasmids were subjected to immunoprecipitation. As clearly shown in Figure 5A, HES1 was co-immunoprecipitated with FLAG-HEN2. Consistent with these results, reciprocal experiments showed that the anti-Myc tag immunoprecipitates contain FLAG-HEN2. *In vitro* pull-down assay demonstrated that radio-labeled FLAG-HEN2 is co-immunoprecipitated with Myc-HES1 (Figure 5B). Additional immunoprecipitation experiments demonstrated that LMO3 also forms a stable complex with HES1 (Figure 6A). We have previously showed that LMO3 forms a stable complex with HEN2 [7]. To investigate the effect of LMO3 on binding of HEN2 and HES1 to putative HES1-binding sites and E-box,

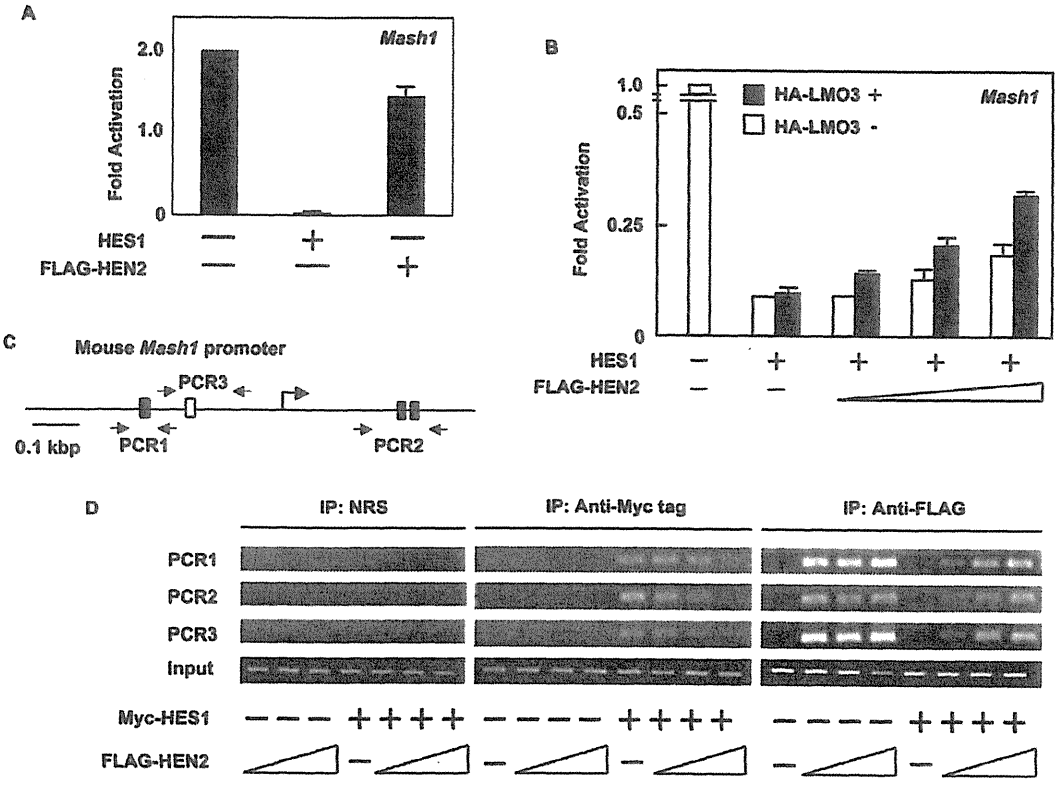

Figure 4. LMO3/HEN2 attenuates HES1-dependent down-regulation of Mash1. (A) Luciferase reporter assay. Neuro2a cells were co-transfected with constant amount of pluc-hMash1 (100 ng), pRL-CMV (0.2 ng) and expression plasmid for HES1 (50 ng) or HEN2 (50 ng). Forty-eight hours after transfection, cells were lysed and their luciferase activities were examined. (B) Luciferase reporter assay. Neuro2a cells were co-transfected with constant amount of pluc-hMash1 (100 ng), pRL-CMV (0.2 ng) and expression plasmid for HES1 (5 ng) in the presence or absence of expression plasmid for HA-LMO3 (150 ng) together with or without increasing amounts of FLAG-HEN2 expression plasmid (100, 200 or 300 ng). Forty-eight hours after transfection, cells were lysed and their luciferase activities were examined. (C) Schematic representation of mouse *Mash1* promoter. The canonical HES1-binding sites and E-box were indicated by filled and open boxes, respectively. The positions of primer sets used for chromatin immunoprecipitation (ChIP) assays were also indicated. (D) ChIP assay. Cross-linked chromatin prepared from Neuro2a cells transfected with the indicated combinations of expression plasmids was sonicated and immunoprecipitated with normal rabbit serum (NRS), polyclonal anti-Myc tag or with polyclonal anti-FLAG antibody. The genomic DNA was purified from the immunoprecipitates and amplified by PCR.
doi:10.1371/journal.pone.0019297.g004

Neuro2a cells were transfected with Myc-HES1 or FLAG-HEN2 together with or without HA-LMO3 expression plasmid and subjected to ChIP assay. As shown in Figure 6B, the immunoprecipitates using anti-Myc tag or anti-FLAG tag antibody contained genomic fragments including putative HES1-binding sites as well as E-box. The amount of Myc-HES1 recruited onto HES1-binding sites and E-box decreased in the presence of HA-LMO3. On the other hand, the amount of FLAG-HEN2 recruited onto HES1-binding sites and E-box increased in the presence of HA-LMO3. As shown in Figure 3F, LMO3 interferes with inhibitory effect of HEN2 on Mash1 expression. These suggest that LMO3 may additively interfere with the inhibitory effect of HES1 on *Mash1* expression by promoting binding of HEN2 to HES1-binding sites and E-box. Collectively, it is conceivable that LMO3/HEN2 reduces the inhibitory effect of HES1 on *Mash1* expression through binding to HES1 and thereby blocking its recruitment onto putative HES1-binding sites and E-box (Figure 7 and Figure S3).

Discussion

In this study, we found that *Mash1* is one of transcriptional targets of LMO3/HEN2 transcriptional complex, and its protein product may play an important role in regulation of neuroblastoma cell growth. As described previously [14], *HEN1* as well as its closely related gene *HEN2* encodes bHLH-type transcription factor, which might recognize E-box (5′-CACGTG-3′). On the other hand, HES1 has an intrinsic transcriptional repressor activity [10]. Based on our present results, adenovirus-mediated expression of LMO3/HEN2 significantly induced *Mash1*, and HES1-mediated down-regulation of *Mash1* promoter activity was recovered by co-expression of LMO3 and HEN2. Our ChIP analyses indicated that HES1 binds to HES1-recognition sites and E-box within *Mash1* promoter in the absence of HEN2, whereas HEN2 efficiently inhibits the recruitment of HES1 onto HES1-binding sites and E-box within *Mash1* promoter, suggesting that HES1 occupies HES1-binding sites and E-box to inhibit the promoter activity of *Mash1*. On the other hand, HEN2 formed a complex with HES1 and reduced the amounts of HES1 recruited onto HES1-binding sites as well as E-box to increase the promoter activity of *Mash1* in collaboration with LMO3. Thus, it is likely that the balance between intracellular amounts of HES1 and LMO3/HEN2 might determine expression levels of *Mash1*, and thereby regulating neuroblastoma cell growth.

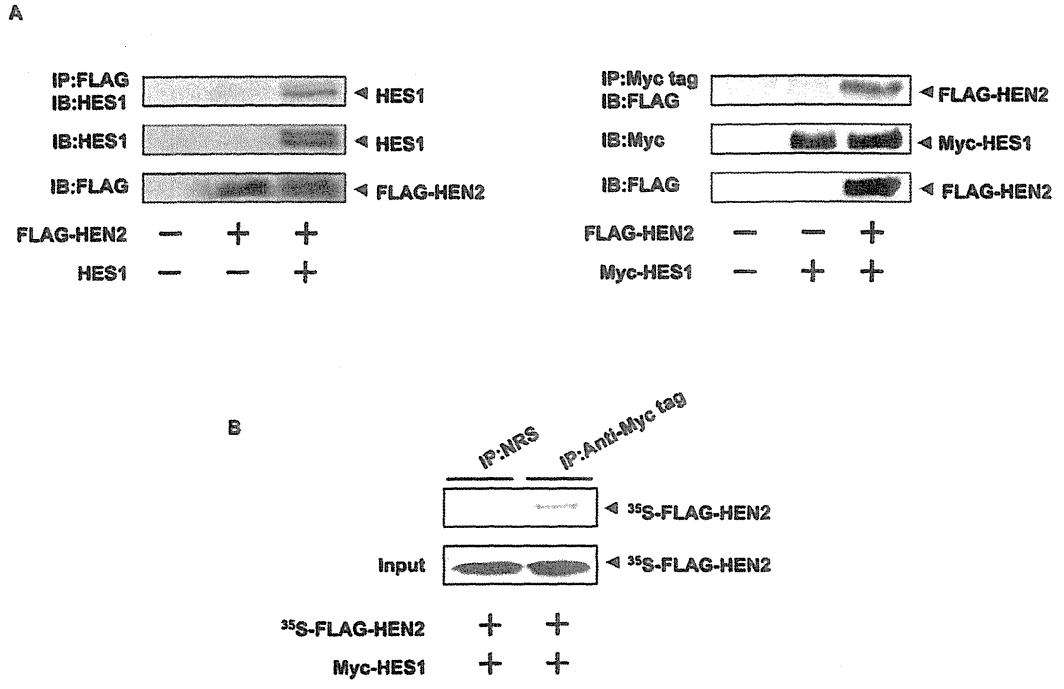

Figure 5. Interaction between HEN2 and HES1 in cells. (A) Neuro2a cells were co-transfected with the indicated combinations of expression plasmids. Forty-eight hours after transfection, cells were lysed and immunoprecipitated with anti-FLAG (left panel) or with anti-Myc tag antibody (right panel) and the immunoprecipitates were analyzed by immunoblotting with anti-HES1 or with anti-FLAG antibody, respectively. Aliquots of cell lysates were subjected to immunoblotting with anti-HES1, anti-FLAG or with anti-Myc tag antibody. (B) *In vitro* pull-down assay. Radio-labeled FLAG-HEN2 was incubated with cell lysates prepared from Neuro2a cells transfected with Myc-HES1 expression plasmid. The reaction mixture was immunoprecipitated with normal rabbit serum (NRS) or with polyclonal anti-Myc tag antibody and separated by SDS-PAGE followed by autoradiography. 1/5 inputs were also shown.
doi:10.1371/journal.pone.0019297.g005

It was reported that de-repression of *Mash1* might interfere with differentiation of sympatho-adrenal precursors of *Insm1* mutant mice although *Mash1* is expressed transiently in those cells during normal neural differentiation [15]. Furthermore, Watt et al. reported that N-myc positively regulates *Mash1* transcription [16]. Therefore, it is possible that in the transcriptional regulation of *Mash1*, LMO3 and HEN2 may associate with other nuclear factors like Insm1 and N-myc besides HES1.

From the developmental point of view, it is known that the LMO/HEN complex plays an important role in regulating neuronal differentiation [11,17]. As described [7,18], expression of *LMO3* was highly restricted in adult and fetal brains, and *HEN2* was expressed in developing nervous system. Genetic studies demonstrated that HEN2 participates in proper neural crest-derived neuroendocrine development and that Mash1 has a critical role in maintaining neuroendocrine cell phenotype [19,20]. Although *LMO3*-knockout mice did not exhibit any significant developmental defects, mice lacking both LMO1 and LMO3 died after birth, which might be due to neural defects [21]. Since neuroblastoma is one of the most common childhood solid tumors of peripheral nervous system arising from as yet unidentified population of neural crest cells [22] and Mash1 regulates proliferation of the sympathetic nervous system [23], it is likely that deregulated expression of Mash1 could contribute to genesis and development of neuroblastoma, which might be regulated by LMO3/HEN2 transcriptional complex both *in vitro* and *in vivo*. This LMO3/HEN2-HES1-Mash1 pathway could be the new future target for developing the anti-neuroblastoma treatment.

Materials and Methods

Ethics Statement

A hundred human neuroblastoma specimens used in the present study were kindly provided from various institutions and hospitals in Japan to the Chiba Cancer Center Neuroblastoma Tissue Bank. Written informed consent was obtained at each institution or hospital. This study was approved by the Chiba Cancer Center Institutional Review Board and were conducted according to the principles expressed in the Declaration of Helsinki.

Tumor Specimens

Tumors were classified according to the International Neuroblastoma Staging System (INSS); 25 Stage 1, 13 Stage 2, 33 Stage 3, 23 Stage 4, and 6 Stage4s. Clinical information including age at diagnosis, tumor origin, Shimada's histology, prognosis, and survival months of each patient were obtained. The median follow-up time for survivors was 35 months (range 3 to 91 months). Each tumor specimen was assayed for *TRKA* expression by Northern blot analysis and for *MYCN* amplification status by both fluorescence in situ hybridization (FISH) and real-time quantitative polymerase chain reaction (PCR).

Quantitative Real-time PCR

Total RNA prepared from primary neuroblastomas was reverse transcribed into cDNA (SuperScript II kit) and subjected to the real-time PCR. The expression level of *GAPDH* was measured in all samples to normalize *LMO3* and *Mash1* expression according to

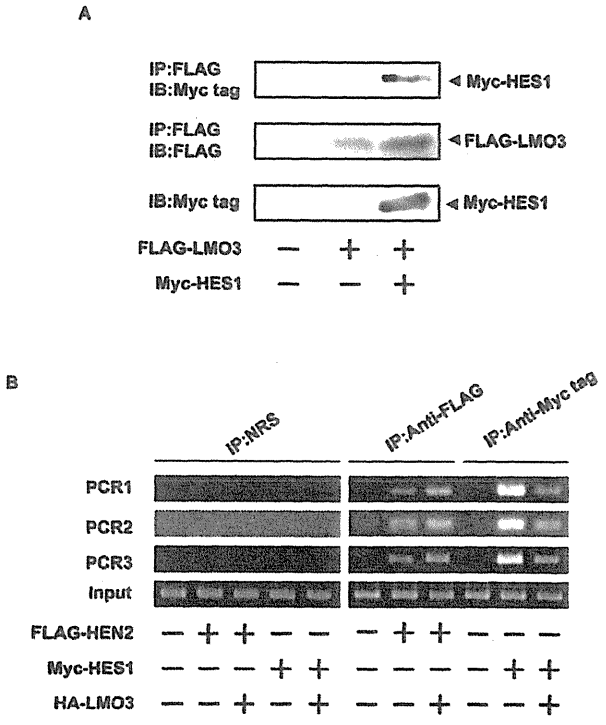

Figure 6. LMO3 attenuates binding of HES1 to Mash1 promoter and promotes that of HEN2. (A) Complex formation between LMO3 and HES1 in cells. Neuro2a cells were transiently transfected with the indicated combinations of the expression plasmids. Forty-eight hours after transfection, cell lysates were immunoprecipitated with anti-FLAG antibody followed by immunoblotting with anti-Myc tag antibody (top panel). Expressions of FLAG-LMO3 and Myc-HES1 are also shown (lower panels). (B) ChIP assay. Cross-linked chromatin prepared from Neuro2a cells transfected with the indicated combinations of expression plasmids was sonicated and immunoprecipitated with normal rabbit serum (NRS), polyclonal anti-Myc tag or with polyclonal anti-FLAG antibody. The genomic DNA was purified from the immunoprecipitates and amplified by PCR.
doi:10.1371/journal.pone.0019297.g006

the manufacturer's instructions (Applied Biosystems, Foster City, CA, USA). Oligonucleotide primers and TaqMan probes, which were labeled at the 5′ end with the reporter dye 6-carboxyfluorescein (FAM) and at the 3′ end with the quencher dye 6-carboxytetramethylrhodamine (TAMRA), were as follows: *LMO3*: forward 5′-TCTGAGGCTCTTTGGTGTAACG-3′, reverse 5′-CCAGGTGGTAAACATTGTCCTTG-3′ and probe 5′-FAM-AAACTGCGCTGCCTGTAGTAAGCTCATCC-TAMRA-3′. Taqman(R) Gene Expression Assay (Applied Biosystems) was purchased for *Mash1* with Assay ID Hs00269932-m1. Amplification and detection were done using the ABI Prism 7700 Sequence Detection System (Applied Biosystems).

Statistical Analysis

Student's *t* tests were used to explore possible associations between *LMO3* expression and other factors. The distinction between high and low levels of *LMO3* and *Mash1* expression was based on the mean value. Kaplan-Meier survival curves were calculated, and survival distributions were compared using the log-rank test. Cox regression models were used to explore associations among *LMO3* expression, *Mash1* expression, age, *MYCN* amplification, tumor origin, Shimada classification and survival. Statistical significance was declared if $P<0.05$.

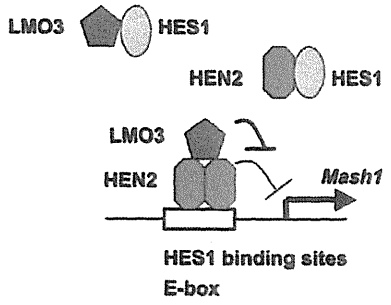

Figure 7. Model for LMO3 and HEN2 cooperation in transcriptional regulation of Mash1 in Neuroblastoma. HES1 binds to HES1 binding sites and E-box on *Mash1* promoter and represses *Mash1* transcription. LMO3 inhibits recruitment of HES1 onto HES1-binding sites and E-box on *Mash1* promoter by forming complex with HES1. HEN2 interferes with recruitment of HES1 onto HES1-binding sites and E-box on *Mash1* promoter by forming complex with HES1 and competing with HES1 in binding to these sites. LMO3 promotes recruitment of HEN2 onto HES1-binding sites and E-box on *Mash1* promoter by forming complex with HEN2 but inhibits negative effects of HEN2 on *Mash1* promoter. Thereby expression of *Mash1* is up-regulated.
doi:10.1371/journal.pone.0019297.g007

Cell Culture and Transfection

SH-SY5Y (human neuroblastoma, ATCC number CRL-2266), SK-N-BE (human neuroblastoma, ATCC number CRL-2271) and Neuro2a (mouse neuroblastoma, ATCC number CCL-131) cells were maintained in RPMI 1640 supplemented with 10% heat-inactivated fetal bovine serum at 37°C in an atmosphere of 5% CO_2 in the air. Cells were transfected with the indicated expression plasmids using Lipofectamine 2000 transfection reagent (Invitrogen, Carlsbad, CA, USA) as recommended by the manufacturer.

Generation of Recombinant Retroviral Vector and Retrovirus-mediated Gene Transfer

Human *Mash1* cDNA was subcloned into the *Hpa*I restriction site of the pLXSN vector. pLXSN or pLXSN- *Mash1* was transfected into the φ2 packaging cells, and SH-SY5Y cells (1×10^6 cells) infected with virus-containing culture medium were cultured in the medium containing 500 μg/ml G418 (Sigma Chemical Co., St. Louis, MO, USA). Two weeks after the selection in G418, drug-resistant clones were isolated and allowed to proliferate in medium containing G418.

Reverse Transcription-PCR Analysis

Total RNA was prepared from cultured cells by using the RNeasy Mini Kit (Qiagen, Valencia, CA, USA). Reverse transcription was carried out using random primers and SuperScript II (Invitrogen). Following the reverse transcription, the resultant cDNA was subjected to PCR-based amplification. PCR primers used were as follows: human *LMO3*, forward 5′-ATGCTCTCAGTCCAGCCAGA-3′ and reverse 5′-TCAGCGAACCTGGGGTGCAT-3′; human *HEN2*, forward 5′-AAGCAGCAGATTCGGACCAT-3′ and reverse 5′-CTTCTCCTCGCGGCTCAG-3′; human *Mash1*, forward 5′-GCGTTCAGCACTGACTTTTG-3′ and reverse 5′-CCCCGGGAGACTTCTTAGAG-3′; human *HES1*, forward 5′-TGAGCCAGCTGAAAACACTG-3′ and reverse 5′-GTCACCTCGTTCATGCACTC-3; human *glyceraldehydes-3-phosphate dehydrogenase* (*GAPDH*), forward 5′-ACCTGACCTGCCGTCTAGAA-3′ and reverse 5′-TCCACCACCCTGTTGCTGTA-3′.

RNA Interference Experiments

Human LMO3 RNAi vector was made using the original plasmid that is gift from A.K. Munirajan (Chiba Cancer Center Research Institute). The targeted sequence is 5′- GTAG-TAAGCTCATCCCTGC -3′. RNAi construct was transiently transfected into SH-SY5Y cells using Lipofectamine 2000 transfection reagent (Invitrogen, Carlsbad, CA, USA) according to the manufacturer's instruction.

Generation of Recombinant Adenoviral Vector

For construction of the adenovirus expression vector, an HA-tagged human LMO3 cDNA or a FLAG-tagged human HEN2 cDNA were inserted into the shuttle vector pHMCMV6 [24]. Efficient construction of a recombinant adenovirus vector by an improved *in vitro* ligation method [25]. The resultant shuttle vector was digested with I-CeuI and PI-SceI and subcloned into the identical restriction sites of the adenovirus expression vector pAdHM4. The recombinant adenovirus construct was digested with *Pac*I and transfected into 293 cells to generate recombinant adenovirus.

Luciferase Reporter Assay

The reporter plasmid contains a 1.2-kb fragment of the human *Mash1* promoter that was subcloned into the pGL3-Basic Vector (Promega Corp., Madison, WI, USA) upstream of the luciferase reporter gene. Cells were seeded in triplicates into 24-well plates (1×10^5 cells/well) 24 h prior to transfection. Cells were cotransfected with 100 ng of the reporter plasmid, 0.2 ng of pRL-CMV encoding *Renilla* luciferase cDNA, 5 ng of rat HES1expression vector, 150 ng of HA-LMO3, 100 to 300 ng of FLAG-HEN2 expression vectors. Total amount of plasmid DNA per transfection was kept constant with pcDNA3 (Invitrogen). At 48 h after transfection, luciferase activity was measured by a Dual-Luciferase Reporter Assay System (Promega), and the transfection efficiency was standardized against *Renilla* luciferase activity.

Chromatin Immunoprecipitation (ChIP) Assays

ChIP assay was performed according to the protocol recommended by Upstate (Lake Placid, NY, USA). Cross-linked chromatin prepared from Neuro2a cells transfected with expression plasmids was sonicated and immunoprecipitated with normal rabbit serum (NRS), polyclonal anti-Myc tag (Medical & Biological Laboratories, Nagoya, Japan) or with polyclonal anti-FLAG (Sigma, St. Louis, MO, USA) antibody. The genomic DNA was purified from the immunoprecipitates and amplified by PCR.

The primers used to amplify the mouse *Mash1* promoters were as follows: HES1 binding site (PCR-1), forward 5′-ATTTCTA-GAGCCACCCCCTG-3′ and reverse 5′-TTGTTGCAGTGCG-TGCGCC-3′; HES1 binding site (PCR-2), forward 5′-AGTGCGCTCGGCACTGACTT-3′ and reverse 5′-CGCG-GTTGGCTTCGGGAGCC-3′; E-box (PCR-3), forward 5′-ATGGAGAGTTTGCAAGGAGC-3′ and reverse 5′-CAGCCC-CACGCGCAGCCCTG-3′.

Western Blot Analysis and Immunoprecipitation

After transfection, Neuro2a cells were placed on ice, washed twice with phosphate-buffered saline, and lysed in lysis buffer containing 25 mM Tris-HCl (pH 8.0), 137 mM NaCl, 2.7 mM KCl, 1% TritonX-100, 1 mM phenylmethylsulfonyl fluoride and protease inhibitor mixture (Sigma). Lysates were placed on ice for 30 min, sonicated briefly, and clarified by centrifugation at 15,000× *g* for 5 min at 4°C. Protein concentrations of the supernatants were determined by using a Bio-Rad protein assay.

For immunoblot analysis, proteins were resolved by sodium dodecyl sulfatepolyacrylamide gel electrophoresis (SDS-PAGE) and electrotransferred onto a nitrocellulose membrane. The membrane filter was blocked with 2% gelatin in Tris-buffered saline (TBS) for 3 h at room temperature and then incubated with a primary antibody including monoclonal anti-rat HES1 (Medical & Biological Laboratories, Nagoya, Japan), monoclonal anti-FLAG (M2; Sigma) or monoclonal anti-Myc (9B11; Cell Signaling Technology, Danvers, MA, USA) antibody over night at 4°C. The membrane filter was then incubated with a goat anti-mouse secondary antibody conjugated to horseradish peroxidase (Cell Signaling Technology, Danvers, MA, USA) or goat anti-rat secondary antibody conjugated to horseradish peroxidase (Beckman Coulter, Marseille, France) for 1 h at room temperature and bound secondary antibody was detected by enhanced chemiluminescence (Amersham Pharmacia Biotech) according to the manufacturer's protocol. For Immunoprecipitation, equal amounts of cell lysates (2 mg) were precleared with 25 µl of protein G-Sepharose (Amersham Bioscience, Uppsala, Sweden). After brief centrifugation, immunoprecipitation was carried out by incubating the supernatant with anti-FLAG polyclonal (Sigma, St. Louis, MO, USA) or anti-Myc tag polyclonal antibody (Medical & Biological Laboratories, Nagoya, Japan) over night at 4°C. Immunocomplexes were precipitated with protein G-Sepharose beads (Amersham Biosciences) for 3 hours at 4°C. The immunoprecipitated proteins were resolved by SDS-PAGE and analyzed by Western blotting.

In vitro Pull-down Assay

Radio-labeled FLAG-HEN2 was generated by using *in vitro* transcription/translation system (Promega) and incubated with cell lysates prepared from Neuro2a cells transfected with Myc-HES1 expression plasmid. The reaction mixture was immunoprecipitated with normal rabbit serum (NRS) or with polyclonal anti-Myc tag antibody (Medical & Biological Laboratories, Nagoya, Japan) and separated by SDS-PAGE followed by autoradiography.

Data Analysis and Statistics

All values for statistical significance represent mean ± SD. We carried out comparisons between means using the Student's *t*-test. Statistical significance implies $P<0.05$.

Supporting Information

Figure S1 Mash1-mediated growth promotion and LMO3/HEN2-mediated transcriptional induction of *Mash1* in SK-N-BE cells. (A) siRNA-mediated knockdown of LMO3. SK-N-BE cells were transfected with empty plasmid (4 µg) or with expression plasmid for siRNA targeting LMO3 (4 µg). Forty-eight hours after transfection, total RNA was prepared and analyzed for expression levels of *LMO3* and *Mash1* by RT-PCR. (B) Decreased growth rate in LMO3-knocked down cells. SK-N-BE cells (4.5×10^3 cells/well, 96 well culture plate) were transfected with empty plasmid (0.2 µg) or with expression plasmid for siRNA targeting LMO3 (0.2 µg). Forty-eight hours after transfection, cells were transferred into fresh medium. At the indicated time points, cell growth was measured by MTT assay (Cell Counting Kit-8, DOJINDO). (C) RT-PCR. SK-N-BE cells were transfected with pcDNA3 empty plasmid or with the indicated combinations of expression plasmid HA-LMO3 or FLAG-HEN2. At 72 hours after transfection, total RNA was analyzed for expression levels of *LMO3*, *HEN2* and *Mash1* by RT-PCR. *GAPDH* was used as an internal control. (D) siRNA-mediated knockdown of LMO3 reduces the promoter activity of *Mash1*. SK-N-BE cells were co-

transfected with constant amount of pluc-Mash1 (100 ng) and pRL-CMV (0.2 ng) in the presence or absence of increasing amounts of expression plasmid for siRNA against human LMO3 (100 or 400 ng). Forty-eight hours after transfection, cells were lysed and their luciferase activities were measured.
(TIF)

Figure S2 Expression of *LMO3*, *HEN2*, *Mash1* or *HES1* in neuroblastoma cell lines. Semiquantitative RT-PCR analysis for expression of *LMO3*, *HEN3*, *Mash1* or *HES1* in neuroblastoma cell lines is performed under linear amplification conditions. Expression of *GAPDH* is shown as a control.
(TIF)

Figure S3 Model for LMO3 and HEN2 cooperation in transcriptional regulation of *Mash1* in Neuroblastoma. (A) HES1 binds to HES1 binding sites and E- box on *Mash1* promoter and represses *Mash1* transcription. (B) LMO3 inhibits recruitment of HES1 onto HES1-binding sites and E-box on *Mash1* promoter by forming complex with HES1, and thereby inducing the expression of Mash1. (C) HEN2 interferes with recruitment of HES1 onto HES1-binding sites and E-box on *Mash1* promoter by forming complex with HES1 and competing with HES1 in binding to these sites. HEN2 also represses *Mash1* transcription but the inhibitory effects are weaker than that of HES1, and so up-regulating transcription of *Mash1*. (D) LMO3 promotes recruitment of HEN2 onto HES1-binding sites and E-box on *Mash1* promoter by forming complex with HEN2 but inhibits negative effects of HEN2 on *Mash1* promoter. Furthermore, LMO3 inhibits recruitment of HES1 onto HES1-binding sites and E-box on *Mash1* promoter, and so *Mash1* may be more highly expressed.
(TIF)

Table S1 Correlation between expression of LMO3 or Mash1 and other prognostic factors (Student's *t*-test).
(PDF)

Table S2 Univariate and multivariate analyses of Mash1 and LMO3 mRNA expression as well as other prognostic factors in primary neuroblastomas.
(PDF)

Acknowledgments

We are grateful to Dr. Ryuichiro Kageyama for providing the expression plasmid encoding HES1, to Drs. Nobutaka Hattori and Kaori Shiba for their valuable discussions. We also thank Yuki Nakamura for her technical assistance.

Author Contributions

Conceived and designed the experiments: EI AN. Performed the experiments: EI. Analyzed the data: EI MO SO. Contributed reagents/materials/analysis tools: YN AN. Wrote the paper: EI MO TO AN.

References

1. Nakagawara A (2004) Neural crest development and neuroblastoma: the genetic and biological link. In: Aloe L, Calzà L, eds. NGF and related molecules in health and disease, Progress in brain research. ELSEVIER. pp 14633–242.
2. Nakagawara A, Ohira M (2004) Comprehensive genomics linking between neural development and cancer: neuroblastoma as a model. Cancer Letters 204: 213–224.
3. Bach I (2000) The LIM domain: regulation by association. Mech Dev 91: 5–17.
4. Rabbitts TH (1998) LMO T-cell translocation oncogenes typify genes activated by chromosomal translocations that alter transcription and developmental processes. Genes Dev 12: 2651–2657.
5. Visvader JE, Venter D, Hahm K, Santamaria M, Sum EY, et al. (2001) The LIM domain gene LMO4 inhibits differentiation of mammary epithelial cells in vitro and is overexpressed in breast cancer. Proc Natl Acad Sci USA 98: 14452–14457.
6. Sum EY, Segara D, Duscio B, Bath ML, Field AS, et al. (2005) Overexpression of LMO4 induces mammary hyperplasia, promotes cell invasion, and is a predictor of poor outcome in breast cancer. Proc Natl Acad Sci USA 102: 7659–7664.
7. Aoyama M, Ozaki T, Inuzuka H, Tomotsune D, Hirato J, et al. (2005) LMO3 interacts with neuronal transcription factor, HEN2, and acts as an oncogene in neuroblastoma. Cancer Res 65: 4587–4597.
8. Gestblom C, Grynfeld A, Ora I, Ortoft E, Larsson C, et al. (1999) The basic helix-loop-helix transcription factor dHAND, a marker gene for the developing human sympathetic nervous system, is expressed in both high- and low-stage neuroblastomas. Lab Invest 79: 67–79.
9. Ichimiya S, Nimura Y, Seki N, Ozaki T, Nagase T, et al. (2001) Downregulation of hASH1 is associated with the retinoic acid-induced differentiation of human neuroblastoma cell lines. Med Pediatr Oncol 36: 132–134.
10. Kageyama R, Ohtsuka T, Kobayashi T (2007) The Hes family: repressors and oscillators that orchestrate embryogenesis. Development 134: 1243–1251.
11. Ramain P, Khechumian R, Khechumian K, Arbogast N, Ackermann C, et al. (2000) Interactions between chip and the achaete/scute-daughterless heterodimers are required for pannier-driven proneural patterning. Mol Cell 6: 781–790.
12. Asmar J, Biryukova I, Heitzler P (2008) *Drosophila* dLMO-PA isoform acts as an early activator of *achaete/scute* proneural expression. Developmental biology 316: 487–497.
13. Axelson H (2004) The Notch signaling cascade in neuroblastoma: role of the basic helix-loop-helix proteins HASH-1 and HES-1. Cancer Letters 204: 171–178.
14. Brown L, Baer R (1994) HEN1 encodes a 20-kilodalton phosphoprotein that binds an extended E-box motif as a homodimer. Mol Cell Biol 14: 1245–1255.
15. Wildner H, Gierl MS, Strehle M, Pla P, Birchmeier C (2008) Insm1 (IA-1) is a crucial component of the transcriptional network that controls differentiation of the sympatho-adrenal lineage. Development 135: 473–481.
16. Watt F, Watanabe R, Yang W, Agren N, Arvidsson Y, et al. (2007) A novel MASH1 enhancer with N-myc and CREB-binding sites is active in neuroblastoma. Cancer Gene Therapy 14: 287–296.
17. Bao J, Talmage DA, Role LW, Gautier J (2000) Regulation of neurogenesis by interactions between HEN1 and neuronal LMO proteins. Development 127: 425–435.
18. Bagley CG, Lipkowitz S, Gobel V, Mahon KA, Bertness V, et al. (1992) Molecular characterization of NSCL, a gene encoding a helix-loop-helix protein expressed in the developing nervous system. Proc Natl Acad Sci USA 89: 38–42.
19. Good DJ, Porter FD, Mahon KA, Parlow AF, Westphal H, et al. (1997) Hypogonadism and obesity in mice with a targeted deletion of the Nhlh2 gene. Nat Genet 15: 397–401.
20. Lanigan TM, DeRaad SK, Russo AF (1998) Requirement of the MASH-1 transcription factor for neuroendocrine differentiation of thyroid C cells. J Neurobiol 34: 126–134.
21. Tse E, Smith AJ, Hunt S, Lavenir I, Forster A, et al. (2004) Null mutation of the Lmo4 gene or a combined null mutation of the Lmo1/Lmo3 genes causes perinatal lethality, and Lmo4 controls neural tube development in mice. Mol Cell Biol 24: 2063–2073.
22. Brodeur GM (2003) Neuroblastoma: biological insights into a clinical enigma. Nat Rev Cancer 3: 203–216.
23. Morikawa Y, Zehir A, Maska E, Deng C, Schneider MD, et al. (2009) BMP signaling regulates sympathetic nervous system development through Smad 4-dependent and -independent pathways. Development 136: 3575–3584.
24. Mizuguchi H, Kay MA (1998) Efficient construction of a recombinant adenovirus vector by an improved *in vitro* ligation method. Hum Gene Ther 9: 2577–2583.
25. Mizuguchi H, Kay MA (1999) A simple method for constructing E1- and E1/E4-deleted recombinant adenoviral vectors. Hum Gene Ther 10: 2013–2017.

VOLUME 29 · NUMBER 24 · AUGUST 20 2011

JOURNAL OF CLINICAL ONCOLOGY

ORIGINAL REPORT

Clinical and Biologic Features Predictive of Survival After Relapse of Neuroblastoma: A Report From the International Neuroblastoma Risk Group Project

Wendy B. London, Victoria Castel, Tom Monclair, Peter F. Ambros, Andrew D.J. Pearson, Susan L. Cohn, Frank Berthold, Akira Nakagawara, Ruth L. Ladenstein, Tomoko Iehara, and Katherine K. Matthay

Wendy B. London, Children's Oncology Group Statistics and Data Center and Dana-Farber Children's Hospital Cancer Center, Boston, MA; Victoria Castel, Unidad de Oncologia Pediatrica Hospital Universitario La Fe, Valencia, Spain; Tom Monclair, Oslo University Hospital, Oslo, Norway; Peter F. Ambros and Ruth L. Ladenstein, Children's Cancer Research Institute, St Anna Kinderkrebsforschung, Vienna, Austria; Andrew D.J. Pearson, Institute of Cancer Research and Royal Marsden Hospital, Surrey, United Kingdom; Susan L. Cohn, The University of Chicago, Chicago, IL; Frank Berthold, University Children's Hospital of Cologne, Germany; Akira Nakagawara, Chiba University, Chiba; Tomoko Iehara, Prefectural Medical University, Kyoto, Japan; and Katherine K. Matthay, University of California San Francisco School of Medicine, San Francisco, CA.

Submitted January 10, 2011; accepted May 26, 2011; published online ahead of print at www.jco.org on July 18, 2011.

Supported in part by the Little Heroes Pediatric Cancer Foundation and Forbeck Foundation (W.B.L.); by Grants No. FIS 09/02323 and GVBE10/08 from Generalitat Valenciana (V.C.); and by National Cancer Institute Grant No. PO1 81403, the Dougherty Foundation, the Conner Fund, and the Alex Lemonade Foundation (K.K.M.).

W.B.L. and V.C. contributed equally to this work.

Authors' disclosures of potential conflicts of interest and author contributions are found at the end of this article.

Corresponding author: Victoria Castel, Unidad de Oncologia Pediatrica, Hospital Universitario La Fe, 46009 Valencia, Spain; e-mail: castel_vic@gva.es.

0732-183X/11/2924-3286/$20.00

DOI: 10.1200/JCO.2010.34.3392

ABSTRACT

Purpose
Survival after neuroblastoma relapse is poor. Understanding the relationship between clinical and biologic features and outcome after relapse may help in selection of optimal therapy. Our aim was to determine which factors were significantly predictive of postrelapse overall survival (OS) in patients with recurrent neuroblastoma—particularly whether time from diagnosis to first relapse (TTFR) was a significant predictor of OS.

Patients and Methods
Patients with first relapse/progression were identified in the International Neuroblastoma Risk Group (INRG) database. Time from study enrollment until first event and OS time starting from first event were calculated. Cox regression models were used to calculate the hazard ratio of increased death risk and perform survival tree regression. TTFR was tested in a multivariable Cox model with other factors.

Results
In the INRG database (N = 8,800), 2,266 patients experienced first progression/relapse. Median time to relapse was 13.2 months (range, 1 day to 11.4 years). Five-year OS from time of first event was 20% (SE, ± 1%). TTFR was statistically significantly associated with OS time in a nonlinear relationship; patients with TTFR of 36 months or longer had the lowest risk of death, followed by patients who relapsed in the period of 0 to less than 6 months or 18 to 36 months. Patients who relapsed between 6 and 18 months after diagnosis had the highest risk of death. TTFR, age, International Neuroblastoma Staging System stage, and *MYCN* copy number status were independently predictive of postrelapse OS in multivariable analysis.

Conclusion
Age, stage, *MYCN* status, and TTFR are significant prognostic factors for postrelapse survival and may help in the design of clinical trials evaluating novel agents.

J Clin Oncol 29:3286-3292. © 2011 by American Society of Clinical Oncology

INTRODUCTION

Neuroblastoma is a genetically and clinically heterogeneous childhood malignancy arising from the embryonic sympathetic nervous system. Neuroblastoma is metastatic at diagnosis in approximately 50% of patients; more than half of children diagnosed with high-risk neuroblastoma will either not respond to conventional therapies or relapse after treatment, necessitating development of novel treatments. Little is known about how to identify patients who are more likely to respond to therapies and survive longer after primary treatment failure in such a heterogeneous disease. Selection of appropriate therapy is one way in which improved outcome can be achieved, so it is crucial to understand the clinical course of neuroblastoma after failure of conventional therapy.

The length of time from diagnosis to first relapse has been demonstrated to be of prognostic value in multiple types of pediatric tumors.[1-5] In one recent single-institution study of high-risk neuroblastoma, time to first relapse was shown to influence length of survival[6]; however, the relationship between initial tumor biologic and clinical risk factors was not extensively studied with regard to the length of second remission and survival after relapse. To gather additional information about the disease course after relapse, we queried the International Neuroblastoma Risk Group (INRG) database. The INRG project is a collaborative effort among cooperative pediatric oncology groups from Europe,

North America, Germany, Australia, New Zealand, and Japan. For the first time, we have a sufficiently large group of annotated relapsed or progressing patients with neuroblastoma to use to identify which clinical and biologic factors are most prognostic of postrelapse survival.[7] In this analysis of 2,266 patients with neuroblastoma who suffered relapse or progression, we show that time to first relapse is significantly associated with survival after relapse, in addition to several other biologic and clinical risk factors in multivariable analysis. This information may help guide therapeutic decisions and interpretation of clinical trials of novel agents.

PATIENTS AND METHODS

INRG Database

A total of 8,800 unique patients younger than 21 years of age with pathologically confirmed neuroblastoma who were diagnosed/enrolled between 1990 and 2002 comprise the INRG database.[7] An enrollment cutoff of 2002 was chosen to allow for sufficient follow-up time. Patients provided consent and were enrolled shortly after initial diagnosis onto one or more neuroblastoma clinical or biologic trials in Germany, Japan, Italy, Spain, or the United Kingdom or onto a North American Children's Oncology Group study or the European SIOP LNESG1 (International Society of Pediatric Oncology Localized Neuroblastoma European Study) trial. Institutional review board approval and informed patient consent were obtained by each country, cooperative group, and treating institution for their respective studies. In addition to date of diagnosis and follow-up data, information on 35 potential risk factors was included in the INRG database.[7] Of the 8,800 patients, the analytic cohort for this report is composed of 2,266 who experienced at least one event (relapse or progression of neuroblastoma or secondary malignancy) and who had available follow-up data. The only other analytic cohort inclusion requirement was that the first event was not death; patients who died at time of relapse/progression were excluded because their OS time could not be calculated. We are interested in patients who require a postrelapse treatment decision.

Statistical Considerations

Time to first event was calculated as time from study enrollment to first occurrence of relapse, progression, or secondary malignancy or time of last patient contact if no event occurred. Overall survival (OS) time was calculated from first event until death or time of last contact if the patient was alive. For ease of discussion, throughout this article, we will refer to these concepts as time to first relapse (TTFR) and OS post relapse, respectively. The method of Kaplan-Meier was used to generate survival curves, and curves were compared using a two-sided log-rank test.[8] OS post relapse is presented as the 5-year point estimate (± SE; per method of Peto et al[9]).

The clinical and biologic factors at diagnosis analyzed are listed in Table 1.[7,10] For lactate dehydrogenase (LDH) and ferritin, median values from the entire INRG cohort (580 units/L and 96 ng/mL, respectively) were used to dichotomize patients as elevated or not elevated. We then chose to use data-driven splits in the risk to construct a survival tree rather than traditional predefined risk groups.

A Cox proportional hazards regression model was used to calculate the hazard ratio (HR) for increased risk of death (poor outcome category as compared with better outcome category).[11] Visual inspection of Kaplan-Meier curves and plots of log(-log(S(t))) versus log(t) were used to identify violations of the proportional hazards assumption.[12] Where the proportional hazards assumption was violated, Cox regression modeling was performed using time-dependent covariates to adjust for nonproportionality. Patients were categorized into 6-month cohorts (0 to < 6, 6 to < 12, 12 to < 18, 18 to < 24, 24 to < 30, 30 to < 36, and ≥ 36 months) of TTFR for graphical presentation of the nonlinear relationship between TTFR and OS post relapse. Time-dependent covariates are somewhat analogous to the use of a squared term in an algebraic equation; to approximate the curve in Figure 2, we included a term for TTFR multiplied by OS time and a binary term for TTFR (< 365 *v* ≥ 365 days) in the Cox model. Inclusion of these terms in the model ensured that patients who progressed within a short time were weighted differently than those who relapsed after therapy.

Cox proportional hazards regression models were used to identify the most highly statistically significant variable to create a given split or branch in the survival tree,[11-14] and only the Table 1 variables that were statistically significant were tested in the survival tree. To account for the effect of TTFR, each step of the model included TTFR time-dependent covariates; these covariates were retained in all models regardless of their statistical significance. *P* values less than .05 were considered statistically significant.[15]

RESULTS

The clinical and biologic characteristics at diagnosis of the 2,266 relapsed/progressing patients are listed in Table 1. Seventy-three percent of patients were 18 months of age or older at diagnosis, 72% had stage 4 tumors, and 33% had *MYCN* amplified tumors. The median TTFR was 13.2 months (range, 1 day to 11.4 years), and for patients with *MYCN* amplified tumors (n = 562) or *MYCN* nonamplified tumors (n = 1,141), it was 11 months (range, 3 days to 7 years) and 14.5 months (range, 7 days to 11 years), respectively ($P < .001$).

Univariate Survival Analyses

The 5-year OS post relapse was 20% (± SE, 1%; n = 2,266; Fig 1A). The median follow-up time of patients who did not die post relapse was 3.6 years (range, 1 day to 13.7 years). Most factors were statistically significantly associated with OS post relapse (Table 1), including unfavorable histology, stage 4, *MYCN* amplification, use of intensive multimodality treatment at diagnosis, age 547 days or older, elevated LDH, elevated ferritin, and high mitosis karyorrhexis index ($P < .001$; HR, ≥ 1.9; Table 1).

TTFR was statistically significantly associated with OS time (Table 2), and a nonlinear relationship was identified (Fig 2). Traditional log-rank test comparisons of short versus long TTFR were not supported, because the required proportional hazards assumption was violated (eg, Fig 1B, using 365-day cutoff), regardless of the choice of the cutoff used to categorize patients as short versus long TTFR. TTFR had an effect on OS post relapse, but the strength of the effect varied for different lengths of TTFR (Fig 2). Each of the 6-month TTFR groups had a higher risk of death after relapse than patients with TTFR of 36 months or longer.

Patients at the highest risk of death were those who relapsed between 6 and 18 months after diagnosis (peak risk at approximately 12 months). Of patients who relapsed 12 months or longer after diagnosis, 24% underwent stem-cell transplantation during initial therapy, compared with only 10% who relapsed in less than 12 months. The risk of death is approximately the same (approximately 2.5 times higher than in patients with TTFR ≥ 36 months) for patients who relapsed within 6 months as it was for patients who relapsed in 18 to less than 24 months. The group of children who relapsed within 6 months after diagnosis included an unexpectedly high proportion of patients with favorable risk factors. Of 461 children who relapsed within 6 months, 55% (255 of 461 patients) were younger than 18 months old at diagnosis in comparison with 20% (362 of 1,805 patients) of those who relapsed later than 6 months after diagnosis ($P < .001$; Appendix Table A1, online only). Similarly, 49% (219 of 448 patients) in the early relapse group had INSS stage 1, 2, 3, and 4S tumors, compared with only 23% of those (403 of 1,752 patients) who

Table 1. Clinical and Genetic Characteristics and Postrelapse Survival in the Relapsed INRG Cohort (n = 2,266)

Factor	Patients		Postrelapse OS		5-Year Postrelapse OS	Postrelapse OS *P*†
	No.	%	HR*	95% CI	OS ± SE (%)	
Histologic classification‡			4.5	3.6 to 5.8		< .001
Favorable	246	27			66 ± 5	
Unfavorable	653	73			11 ± 2	
INSS stage			3.5	3.1 to 4.0		< .001
1, 2, 3, 4S	622	28			52 ± 3	
4	1,578	72			8 ± 1	
MYCN status			2.7	2.4 to 3.1		< .001
Nonamplified	1,141	67			32 ± 2	
Amplified	562	33			7 ± 2	
Initial treatment			2.6	2.3 to 2.9		< .001
Observation, surgery, or standard chemotherapy	762	40			41 ± 3	
Intensive multimodality	1,143	60			7 ± 1	
Age, days			2.4	2.1 to 2.7		< .001
< 547	617	27			47 ± 3	
≥ 547	1,649	73			10 ± 1	
LDH, U/L			2.4	2.1 to 2.8		< .001
< 580	466	35			38 ± 2	
≥ 580	848	65			12 ± 2	
Serum ferritin, ng/mL			2.1	1.8 to 2.4		< .001
< 96	321	28			34 ± 4	
≥ 96	839	72			12 ± 2	
MKI‡			1.9	1.6 to 2.4		< .001
Low, intermediate	550	74			28 ± 3	
High	189	26			12 ± 4	
1p			1.8	1.4 to 2.1		< .001
No loss or aberration	345	58			32 ± 5	
LOH, deletion, or imbalance	252	42			15 ± 3	
Ploidy			1.6	1.4 to 2.0		< .001
> 1 (hyperdiploid)	357	57			34 ± 4	
≤ 1 (diploid, hypodiploid)	273	43			16 ± 4	
Grade of NB differentiation‡			1.6	1.1 to 2.1		< .001
Differentiating	72	9			38 ± 8	
Undifferentiated	774	91			22 ± 3	
Diagnostic category‡						
1 (NB, stroma poor)	992	91			21 ± 2	
2 (GNB, intermixed, stroma rich)	5	0.5			0	
3 (GNB, well differentiated, stroma rich)	5	0.5			0	
4 (GNB, nodular [composite])	90	8			10 ± 7	
2 and 3 *v* 1 and 4			1.4	0.8 to 2.4		.686
2 and 3	10	1			0	
1 and 4	1,082	99			20 ± 2	
Year of diagnosis			1.3	1.2 to 1.4		< .001
≥ 1996	1,333	59			25 ± 3	
< 1996	933	41			17 ± 1	
11q			1.1	0.8 to 1.5		.567
Balanced or no aberration	205	65			35 ± 6	
Deletion, imbalance, or unbalanced	115	35			20 ± 7	
17q			1.1	0.7 to 1.6		.764
No gain	64	41			29 ± 8	
Gain	91	59			23 ± 9	

Abbreviations: GNB, ganglioneuroblastoma; HR, hazard ratio; INPC, International Neuroblastoma Pathology Classification; INRG, International Neuroblastoma Risk Group; INSS, International Neuroblastoma Staging System; LDH, lactate dehydrogenase; LOH, loss of heterozygosity; MKI, mitosis karyorrhexis index; NB, neuroblastoma; OS, overall survival.

*HRs denote increased risk of event for second row within given category as compared with first row.

†Per log-rank test.

‡Per INPC; per Shimada, if INPC missing.

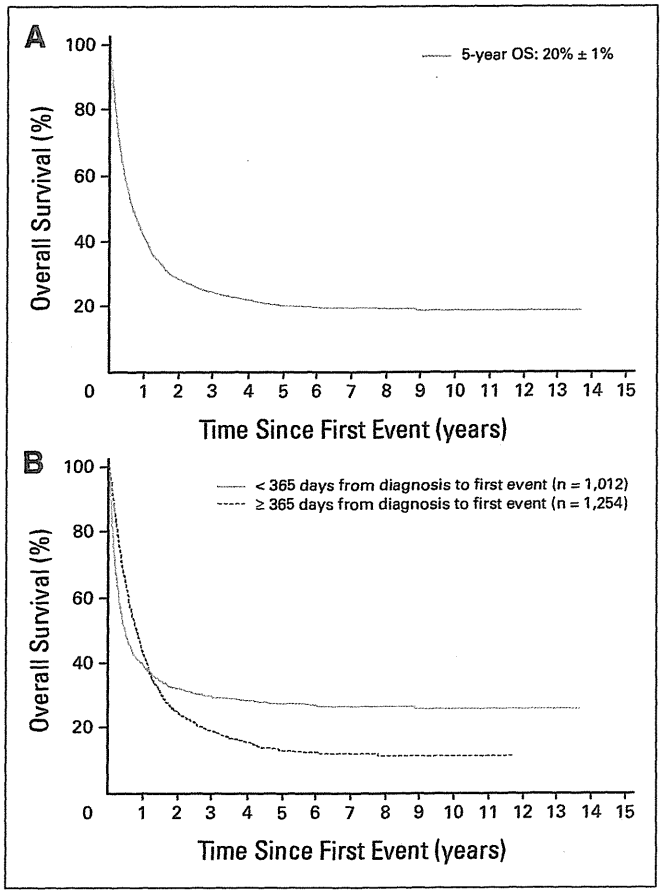

Fig 1. (A) Overall survival post relapse for 2,266 patients with neuroblastoma from the International Neuroblastoma Risk Group database. Median time to first relapse (TTFR) was 13.2 months (range, 1 day to 13.1 years). (B) Overall survival post relapse. TTFR less than 365 days from diagnosis (n = 1,012) versus TTFR 365 days or more from diagnosis (n = 1,254). Log-rank test *P* value is not valid because of violation of proportional hazards assumption, which can be seen in crossing of two curves.

relapsed later than 6 months ($P < .001$; Appendix Table A1, online only). Within the subset of relapsed patients who were stage 3 or 4 and *MYCN* amplified, the nonlinear relationship persisted (Fig 2), with a high risk of death for patients who relapsed within the first 12 months of diagnosis.

Multivariable Survival Analyses

Although many factors were prognostic in a univariate test, few were prognostic in a multivariable Cox model (Table 3). Stage was the most highly predictive of OS post relapse, with increased risk of death for stages 4, 3, and 4S (6.9, 4.3, and 3.5 times higher than stages 1 and 2, respectively), with adjustment for TTFR by simultaneous inclusion in the Cox model.

The survival tree regression models identified a small proportion of patients who may have been salvageable after relapse (Fig 3). In the context of relapse therapy administered from 1990 to 2005, the salvageable cohorts seem to be those with stage 1, 2, 3, or 4S disease who had *MYCN* nonamplified tumors (excluding those with undifferentiated histology); those with stage 4 disease age younger than 18 months who had *MYCN* nonamplified tumors; and those with stage 1, 2, or 4S disease who had *MYCN* amplified tumors. Combined, approximately 15% of relapsed/progressing patients seemed to be curable. Within the survival tree subgroups, there were only two subgroups within which TTFR was statistically significantly associated with OS (ie, stage 4 patients with *MYCN* amplified tumors and stage 3 patients with *MYCN* amplified tumors).

DISCUSSION

TTFR has been demonstrated to be prognostic in different pediatric tumors,[1-5] but it has not been thoroughly studied in neuroblastoma. Some studies have shown that a more chronic course of neuroblastoma after failure of primary therapy seems to be associated with longer times of first remission[16] or older age at diagnosis.[17-19] Cotterill et al[20] identified late relapse in a small subset of high-risk patients; however, this study was unable to predict which factors influence long-term survival given the limited follow-up.

In each of the single-institution studies, the number of patients and data collection were limited. In our analysis of 2,266 patients with relapsed neuroblastoma, we have shown that TTFR is an important factor to predict OS after an event. The relationship of TTFR and OS post relapse is complex; the risk of death was highest for patients who relapsed between 6 and 18 months from diagnosis and then decreased steadily, being lowest in patients who relapsed at 36 months or later. The association of TTFR and OS post relapse was the strongest in stage 3 and 4 patients with *MYCN* amplified tumors. Surprisingly, in the overall cohort, the risk of death for patients who relapsed between 6 and 18 months after diagnosis was higher than for patients who relapsed within 0 to 6 months, or more than 18 months, after diagnosis. A more intuitive relationship would be linear, where those with the shortest TTFR had the highest risk of death, with decreasing risk of death as TTFR increased. A possible explanation for why the patients with the shortest TTFR did not have the highest risk of death may lie in the more favorable clinical characteristics of the patients who relapsed within 6 months; a significantly larger proportion of patients were younger or had stage 1, 2, 3, or 4S disease in comparison with those who relapsed later. Patients who were younger and had a lower stage of disease may have received little or no therapy before relapse and therefore may have responded well to postrelapse treatment. Another possible explanation for the upward slope of the risk-of-death curve with TTFR of less than 12 months and the downward slope of the risk-of-death curve with TTFR of 12 months or longer (Fig 2) is that patients who are able to make it to transplantation (occurring approximately 10 to 12 months post diagnosis) without relapse/progression realize a benefit in terms of prolonged OS.

Accepted prognostic factors for neuroblastoma include age at diagnosis, *MYCN* gene amplification, and histologic features.[21] These factors are standard determinants of initial risk stratification, but their prognostic value after an event had not been studied previously. In our analysis, we identified several factors that were independently prognostic of OS after relapse: stage, *MYCN* status, age, and TTFR. Many other factors were significantly predictive of poor outcome after relapse in univariate, but not multivariable, analysis. Within the subgroups of patients with *MYCN* nonamplified tumors or stage 1, 2, or 4S disease, TTFR was not predictive of OS post relapse; it seems that the patients with INSS stage 3 and 4 *MYCN* amplified tumors were driving the association between TTFR and OS.

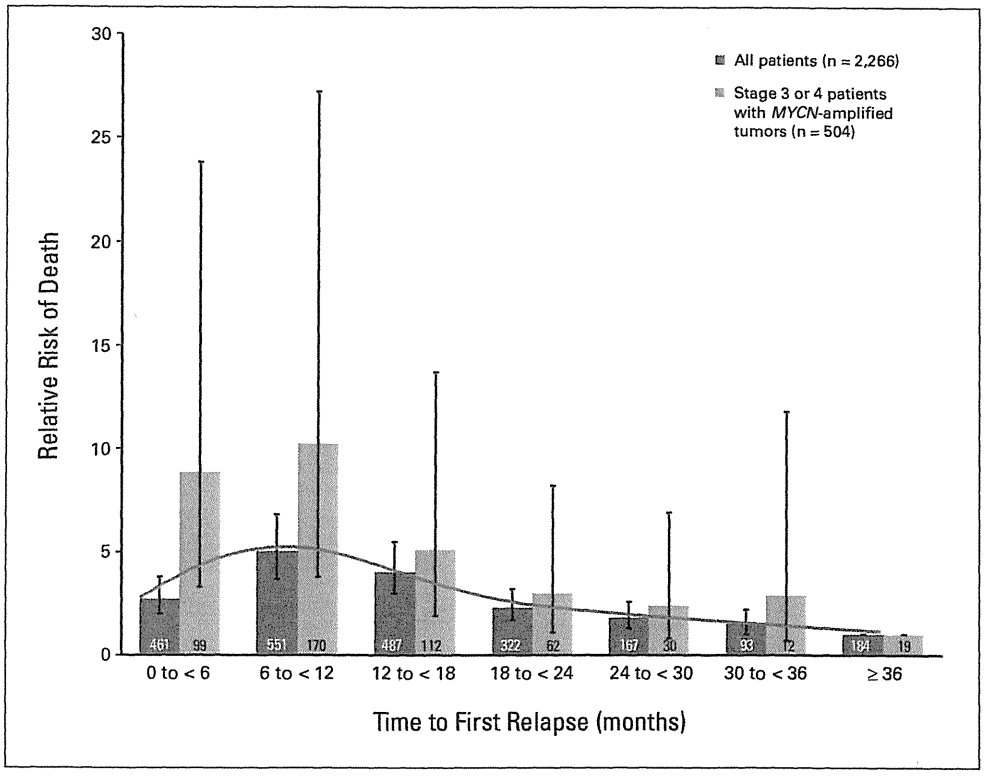

Fig 2. Relative risk (hazard ratio) of death for 6-month cohorts of time to first relapse in comparison with patients whose first relapse occurred more than 36 months from diagnosis. Patients whose first relapse occurred more than 36 months from diagnosis had a relative risk of death equal to 1. Blue bars are all patients (n = 2,266), and gold bars are the subset of stage 3 or 4 patients with *MYCN* amplified tumors (n = 504). SE bars are shown for relative risk of death for each cohort.

Two previous single-institution studies in neuroblastoma also showed that shorter time to first relapse was a significant adverse factor for survival.[6,16] Lau et al[16] reviewed 31 patients with neuroblastoma with relapsed disease and found that patients who relapsed less than 12 months from diagnosis had significantly shorter survival time. The only other significant factor in their analysis for survival post relapse was tumor *MYCN* amplification. Santana et al[6] addressed the study of disease-control intervals in 91 high-risk patients with neuroblastoma. The estimated median times to disease recurrence were 18.3, 8.7, and 3.8 months for the first, second, and third recurrences, respectively. Patients with longer initial disease control had a significant postrecurrence survival advantage. This study emphasized the importance of knowing the intervals of disease progression as end points for the design of protocols with new agents.[6]

Other studies in pediatric malignancies have also shown that earlier relapse portends shorter survival. The Italian Off-Therapy Registry published results on 694 patients, including those with neuroblastoma, CNS tumors, sarcoma, Wilm's tumors, and Hodgkin's lymphoma, who had experienced recurrence. They found significantly different HRs for survival by type of diagnosis and found overall that patients relapsing less than 12 months off therapy had worse survival in univariate, but not in multivariable, analysis.[22] Risk factors for survival post relapse in neuroblastoma

Table 2. Multivariable Analysis of OS After First Event

Time to First Relapse (months)*	No. of Patients	Risk of Death†		
		HR	95% CI	*P*
0 to < 6	461	2.7	2.0 to 3.8	< .001
6 to < 12	551	5.0	3.7 to 6.8	< .001
12 to < 18	487	4.0	3.0 to 5.5	< .001
18 to < 24	322	2.3	1.7 to 3.2	< .001
24 to < 30	167	1.8	1.3 to 2.6	< .001
30 to < 36	93	1.5	1.0 to 2.2	.063
≥ 36	184	1.0	1.0 to 1.0	NA

NOTE. Analysis testing of 6-month categories of time to first relapse compared with risk of death for those relapsing more than 36 months after diagnosis.

Abbreviations: HR, hazard ratio; NA, not applicable; OS, overall survival.

*All 6-month categories were simultaneously included in the model, except for ≥ 36, which was the reference level.

†In comparison with patients with first relapse more than 36 months after diagnosis.

Table 3. Clinical and Biologic Factors Independently Predictive of OS in Multivariable Analysis (n = 2,266)

Variable*	Risk of Death		
	HR	95% CI	*P*
Stage 4	6.9	5.1 to 9.3	< .001
Stage 3	4.3	3.1 to 6.1	< .001
Stage 4S	3.5	2.2 to 5.4	< .001
MYCN amplification	2.4	2.1 to 2.7	< .001
Age ≥ 18 months	1.6	1.4 to 1.9	< .001
TTFR < 12 months	2.0	1.7 to 2.5	< .001
TTFR × OS time†	1.0	1.0 to 1.0	< .001

Abbreviations: HR, hazard ratio; OS, overall survival; TTFR, time to first relapse.

*Variables tested in multivariable model were those significant in survival tree regression: stage, *MYCN* status, age, ploidy, lactate dehydrogenase, and grade of differentiation.

†Interaction term consisting of 12-month TTFR cutoff multiplied by OS time is used to approximate curve shown in Figure 2.

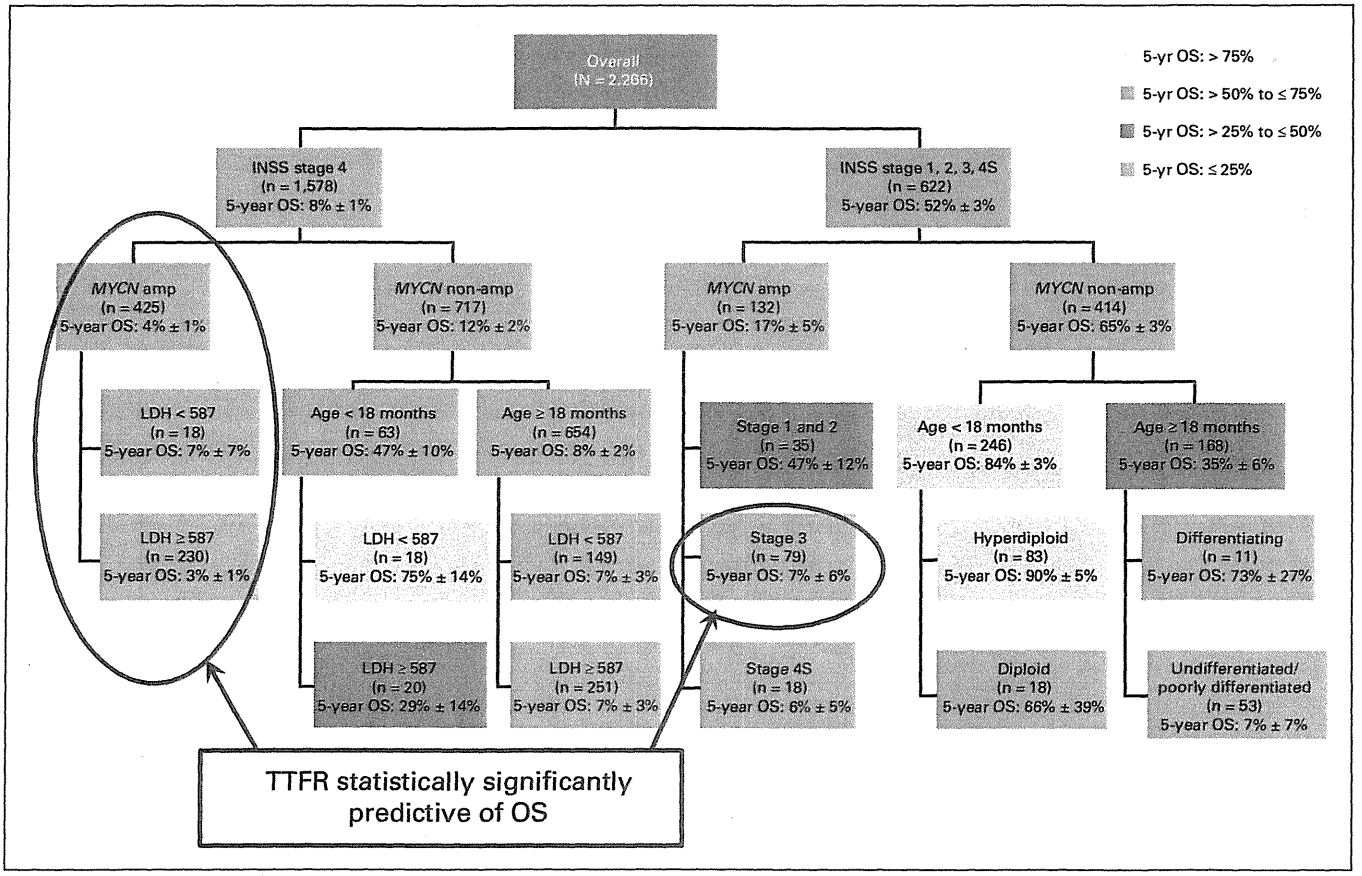

Fig 3. Survival tree regression of overall survival post relapse. Modeling was performed with adjustment for time to first relapse. Within each subgroup box, the value of OS post relapse is presented as the 5-year point estimate (± SE). INSS, International Neuroblastoma Staging System; LDH, lactate dehydrogenase; OS, overall survival; TTFR, time to first relapse.

were not evaluated separately. Interestingly, the patients relapsing in the more recent treatment era had shorter survival, perhaps because the relapse may have occurred after more intensive therapy. A similar trend has been reported in childhood leukemia, in which multiple studies have shown that duration of first remission was the most significant predictor of outcome after relapse of acute lymphoblastic leukemia.[4,5]

In a retrospective study, Garaventa et al[23] described 781 children with neuroblastoma experiencing tumor recurrence. Ten-year OS was 6.8% after progression and 14.4% after relapse. Similar to our series, the factors worsening prognosis in univariate analysis were age older than 18 months, advanced stage, high LDH, *MYCN* amplification, and abdominal primary (no multivariable analysis). Most relapses occurred early (median interval, 7.8 months), but 86 (24%) occurred late (median, 28 months). Early relapses had a more rapid, unfavorable course, with approximately 80% of deaths occurring within 2 years, whereas survival time was longer for late relapses.

From German protocols NB90, NB97, and NB2004 (n = 493 high-risk patients), Simon et al[24] presented data on 254 patients with neuroblastoma who relapsed after autologous bone marrow transplantation as part of initial treatment. *MYCN* amplification, early recurrence within 18 to 24 months after diagnosis, bone marrow, and lung/pleura metastasis at relapse were independently predictive of poor survival. The 24 patients who underwent a second autologous stem-cell transplantation had better outcome.

Ultimately, understanding the genetic differences in early versus late relapsing patients will facilitate selection of appropriate targeted therapy. Meanwhile, we propose that stratification of relapsed patients according to the timing of first relapse, as well as stage, age, and *MYCN* status, is critical in certain types of study designs, such as randomized phase II trials, to maintain a balance of less favorable patients between treatment arms. One might also wish to compare two strata for a given treatment to see which has better outcome. TTFR is a significant, readily available prognostic factor for stratification of patients on retrieval trials. In addition, TTFR may be used in therapy selection. Studies of novel agents using time to progression as an end point could be designed to stratify patients based on TTFR so that the effect of the novel agents can be separated from inherent tumor behavior.

We were not able to establish a single clear TTFR cutoff time point for stratification, perhaps because the INRG series is heterogeneous in relation to era of treatment and initial therapy received or because the true relationship between TTFR and OS post relapse is nonlinear. Our results demonstrate that the period from 6 to 18 months from diagnosis to relapse is associated with the shortest survival of relapsing patients, including the subset of patients with stage 3 and 4 *MYCN* amplified tumors.

In conclusion, time to first relapse is a significant predictor of death after relapse; the risk of death is higher for patients who relapse between 6 and 18 months after diagnosis than it is for patients who relapse more than 18 months from diagnosis. Stratification of relapsed patients with neuroblastoma according to the timing of first relapse,

age, stage, and *MYCN* status is important in retrieval study designs, especially for patients with stage 3 or 4 *MYCN* amplified tumors.

AUTHORS' DISCLOSURES OF POTENTIAL CONFLICTS OF INTEREST

The author(s) indicated no potential conflicts of interest.

AUTHOR CONTRIBUTIONS

Conception and design: Wendy B. London, Victoria Castel, Andrew D.J Pearson, Akira Nakagawara, Katherine K. Matthay

Financial support: Wendy B. London

Administrative support: Wendy B. London, Victoria Castel

Provision of study materials or patients: Victoria Castel, Peter F. Ambros, Frank Berthold, Akira Nakagawara, Ruth L. Ladenstein, Tomoko Iehara

Collection and assembly of data: Wendy B. London, Victoria Castel, Tom Monclair, Peter F. Ambros, Susan L. Cohn, Frank Berthold, Ruth L. Ladenstein, Tomoko Iehara

Data analysis and interpretation: Wendy B. London, Victoria Castel, Andrew D.J Pearson, Katherine K. Matthay

Manuscript writing: All authors

Final approval of manuscript: All authors

REFERENCES

1. Barker LM, Pendergrass TW, Sanders JE, et al: Survival after recurrence of Ewing's sarcoma family of tumors. J Clin Oncol 23:4354-4362, 2005
2. Leavey P, Mascarenhas L, Marina N, et al: Prognostic factors for patients with Ewing sarcoma (EWS) at first recurrence following multi-modality therapy: A report from the Children's Oncology Group. Pediatr Blood Cancer 51:334-338, 2008
3. Dantonello T, Int-Veen C, Winkler P, et al: Initial patient characteristics can predict pattern and risk of relapse in localized rhabdomyosarcoma. J Clin Oncol 26:406-413, 2008
4. Malempati S, Gaynon P, Sather H, et al: Outcome after relapse among children with standard-risk acute lymphoblastic leukemia: Children's Oncology Group study CCG-1952. J Clin Oncol 25:5800-5807, 2007
5. Nguyen K, Devidas M, Cheng S, et al: Factors influencing survival after relapse from acute lymphoblastic leukemia: A Children's Oncology Group study. Leukemia 22:2142-2150, 2008
6. Santana V, Furman W, McGregor L, et al: Disease control intervals in high-risk neuroblastoma. Cancer 112:2796-2801, 2008
7. Cohn S, Pearson A, London W, et al: The International Neuroblastoma Risk Group (INRG) classification system: An INRG Task Force report. J Clin Oncol 27:289-297, 2009
8. Kaplan EL, Meier P: Nonparametric estimation from incomplete observations. J Am Stat Assoc 53: 457-481, 1958
9. Peto R, Pike M, Armitage P, et al: Design and analysis of randomized clinical trials requiring prolonged observation of each patient: I. Introduction and design. Br J Cancer 34:585-612, 1976
10. Ambros PF, Ambros IM, Brodeur GM, et al: International consensus for neuroblastoma molecular diagnostics: Report from the International Neuroblastoma Risk Group (INRG) Biology Committee. Br J Cancer 100:1471-1482, 2009
11. Cox DR: Regression models and life-tables. J R Stat Soc 34:187-220, 1972
12. Segal MR: Regression trees for censored data. Biometrics 44:35-47, 1988
13. Davis RB, Anderson JR: Exponential survival trees. Stat Med 8:947-961, 1989
14. Leblanc M, Crowley J: Survival trees by goodness of split. J Am Stat Assoc 88:457-467, 1993
15. Fleming TR, Harrington DP: Counting Processes and Survival Analysis. New York, NY, John Wiley & Sons, 1991
16. Lau L, Tai D, Weitzman S, et al: Factors influencing survival in children with recurrent neuroblastoma. J Pediatr Hematol Oncol 26:227-232, 2004
17. Kushner BH, Kramer K, Cheung NK: Chronic neuroblastoma. Cancer 95:1366-1375, 2002
18. Franks LM, Bollen A, Seeger RC, et al: Neuroblastoma in adults and adolescents: An indolent course with poor survival. Cancer 79:2028-2035, 1997
19. Conte M, Parodi S, De Bernardi B, et al: Neuroblastoma in adolescents: The Italian experience. Cancer 106:1409-2006;
20. Cotterill SJ, Pearson AD, Pritchard J, et al: Late relapse and prognosis for neuroblastoma patients surviving 5 years or more: A report from the European Neuroblastoma Study Group "Survey." Med Pediatr Oncol 36:235-238, 2001
21. George RE, Variend S, Cullinane C, et al: Relationship between histopathological features, MYCN amplification, and prognosis: A UKCCSG study United Kingdom Children Cancer Study Group. Med Pediatr Oncol 36:169-176, 2001
22. Ceschel S, Casotto V, Valsecchi M, et al: Survival after relapse in children with solid tumors: A follow-up study from the Italian off-therapy registry. Pediatr Blood Cancer 47:560-566, 2006
23. Garaventa A, Parodi S, De Bernardi B, et al: Outcome of children with neuroblastoma after progression or relapse: A retrospective study of the Italian neuroblastoma registry. Eur J Cancer 45:2835-2842, 2009
24. Simon T, Berthold F, Klingenbiel T, et al: Do relapsed high risk neuroblastoma patients have a second chance? Pediatr Blood Cancer 53; 5:736, 2009

VOLUME 29 · NUMBER 33 · NOVEMBER 20 2011

JOURNAL OF CLINICAL ONCOLOGY

ORIGINAL REPORT

Prognostic Value of the Stage 4S Metastatic Pattern and Tumor Biology in Patients With Metastatic Neuroblastoma Diagnosed Between Birth and 18 Months of Age

Denah R. Taggart, Wendy B. London, Mary Lou Schmidt, Steven G. DuBois, Tom F. Monclair, Akira Nakagawara, Bruno De Bernardi, Peter F. Ambros, Andrew D.J. Pearson, Susan L. Cohn, and Katherine K. Matthay

Denah R. Taggart, Steven G. DuBois, and Katherine K. Matthay, University of California San Francisco School of Medicine and Benioff Children's Hospital, San Francisco, CA; Wendy B. London, Dana-Farber Cancer Institute/Children's Hospital, Boston, MA; Mary Lou Schmidt, University of Illinois; Susan L. Cohn, University of Chicago, Chicago, IL; Tom F. Monclair, Rikshospitalet University Hospital, Oslo, Norway; Akira Nakagawara, Chiba Cancer Center, Chiba, Japan; Bruno De Bernardi, Istituto Giannina Gaslini, Genova, Italy; Peter F. Ambros, Children's Cancer Research Institute, St Anna Kinderkrebsforschung, Vienna, Austria; and Andrew D.J. Pearson, Institute of Cancer Research, Sutton, United Kingdom.

Submitted March 15, 2011; accepted July 25, 2011; published online ahead of print at www.jco.org on October 3, 2011.

Supported in part by National Institutes of Health Grant No. T32 CA128583-01, William Guy Forbeck Research Foundation, Dougherty Foundation, Conner Research Fund, Campini Foundation, and Mildred V. Strouss Professorship.

Presented in part at the 45th Annual Meeting of the American Society of Clinical Oncology, May 29-June 2, 2009, Orlando, FL.

Authors' disclosures of potential conflicts of interest and author contributions are found at the end of this article.

Corresponding author: Katherine K. Matthay, MD, Department of Pediatrics, UCSF School of Medicine, 505 Parnassus Ave, Box 0106, San Francisco, CA 94143-0106; e-mail: matthayk@peds.ucsf.edu.

0732-183X/11/2933-4358/$20.00

DOI: 10.1200/JCO.2011.35.9570

ABSTRACT

Purpose
Patients with neuroblastoma younger than 12 months of age with a 4S pattern of disease (metastases limited to liver, skin, bone marrow) have better outcomes than infants with stage 4 disease. The new International Neuroblastoma Risk Group (INRG) staging system extends age to 18 months for the 4S pattern. Our aim was to determine which prognostic features could be used for optimal risk classification among patients younger than 18 months with metastatic disease.

Methods
Event-free survival (EFS) and overall survival were analyzed by log-rank tests, Cox models, and survival tree regression for 656 infants with stage 4S neuroblastoma younger than 12 months of age and 1,019 patients with stage 4 disease younger than 18 months of age in the INRG database.

Results
Unfavorable biologic features were more frequent in infants with stage 4 disease than in infants with 4S tumors and higher overall in those age 12 to 18 months (although not different for stage 4 *v* 4S pattern). EFS was significantly better for infants younger than 12 months with 4S pattern than with stage 4 disease ($P < .01$) but similar for toddlers age 12 to 18 months with stage 4 versus 4S pattern. Among 717 patients with stage 4S pattern, patients age 12 to 18 months had worse EFS than those age younger than 12 months ($P < .01$). *MYCN*, 11q, mitosis-karyorrhexis index (MKI), ploidy, and lactate dehydrogenase were independently statistically significant predictors of EFS and more highly predictive than age or metastatic pattern. *MYCN*, 11q, MKI, histology, and 1p were combined in a survival tree for improved risk stratification.

Conclusion
Tumor biology is more critical than age or metastatic pattern for prognosis of patients age younger than 18 months with metastatic neuroblastoma and should be considered for risk stratification.

J Clin Oncol 29:4358-4364. © 2011 by American Society of Clinical Oncology

INTRODUCTION

Stage 4S neuroblastoma is a unique category of metastatic disease in infants. Originally described in 1971,[1] the definition (clarified by International Neuroblastoma Staging System [INSS]) categorizes infants younger than 12 months of age with metastases limited to the liver, skin, and bone marrow (< 10% replacement with tumor cells) as having stage 4S disease, hereafter referred to as 4S pattern. The primary tumor must be localized (INSS 1 or 2), without infiltration across the midline or contralateral lymph node involvement.[2]

Patients with 4S disease (7% to 10% of neuroblastoma)[3] have a more favorable outcome than other patients with metastatic neuroblastoma, often demonstrating spontaneous maturation and regression. Estimated survival rates of 70% to 90% have been reported, and these tumors are usually associated with favorable biologic features.[4-7] Unfortunately, a subgroup of patients with stage 4S disease and unfavorable prognostic features—including *MYCN* amplification, chromosomal aberrations (loss of heterozygosity [LOH] 1p, aberration 11q, gain 17q), diploidy, and age younger than 2 months at diagnosis—has significantly worse outcomes.[3,4,8-14]

The upper age limit defining 4S disease has been debated as a result of recent reports demonstrating more favorable outcomes for patients with metastatic

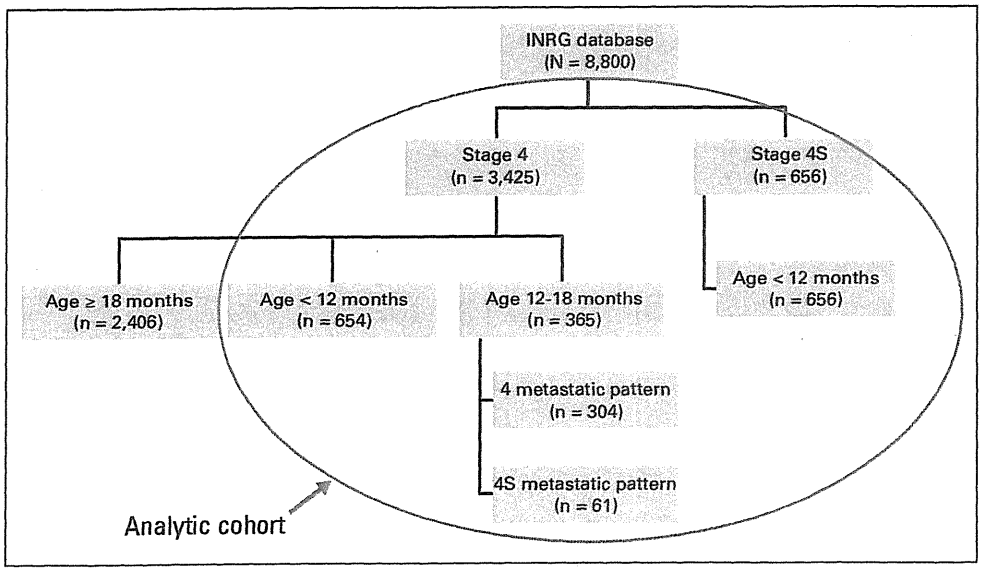

Fig 1. Analytic cohort. INRG, International Neuroblastoma Risk Group.

neuroblastoma diagnosed between 12 and 18 months of age.[15,16] Recently, the International Neuroblastoma Risk Group (INRG) developed consensus guidelines for a modified staging system based on clinical and radiologic criteria. The INRG increased the upper limit of age from 12 to 18 months for 4S disease (now designated Ms), defined as metastases limited to skin, liver, and bone marrow (< 10%) without cortical bone involvement and either L1 or L2 stage tumors, including large unresectable primary tumors that cross the midline.[17] These patients were then stratified by biologic features for risk classification. The current study uses the INRG database of 1,675 patients with metastatic neuroblastoma age 0 to 18 months to determine whether biologic and clinical features better than the younger-than-12-months age cutoff and 4S metastatic pattern can be identified to categorize patients with good outcomes.

METHODS

Patients

The INRG database contains information on 8,800 unique patients who provided consent for and were enrolled onto cooperative clinical trials between January 1, 1990, and December 31, 2002, by cooperative groups from multiple countries.[17] Requirements for eligibility into the INRG database include confirmed pathologic diagnosis of neuroblastoma excluding ganglioneuroma,[18] age 21 years or younger at diagnosis, and available data for disease and survival outcomes.

From this database, we identified 3,425 patients with INSS stage 4 and 656 patients with INSS stage 4S disease (Fig 1). Among patients with stage 4 disease, 654 were age younger than 12 months (infants) and 365 were age 12 to 18 months (toddlers) at diagnosis. With regard to patients with stage 4S disease, all 656 were younger than 12 months of age (by definition). These 1,675 patients formed our analytic cohort. We divided the patients with stage 4 disease age 12 to 18 months into two groups—those with (n = 61) and without (n = 304) 4S pattern of metastasis—independent of size of primary tumor or extent of bone marrow involvement.

Statistical Considerations

Factors evaluated in tests of association and survival analyses were as follows: *MYCN* gene amplification,[19,20] 11q aberration, 1p aberration, ploidy, grade, mitosis-karyorrhexis index (MKI), lactic dehydrogenase (LDH), primary site (adrenal *v* not adrenal), and initial treatment (surgery and observation *v* more intensive therapies). Both 11q and 1p chromosomal abnormalities were detected using fluorescence in situ hybridization or polymerase chain reaction. Using flow cytometry, ploidy was reported as less than or equal to one or more than one; all patients with more than one were classified as hyperdiploid. Histology is often used to categorize tumors as favorable or unfavorable. Because the INPC and Shimada classification systems incorporate age into their categorization, there is a duplication of the prognostic contribution when both age and histology are used as risk factors.[18,21] Therefore, we used tumor grade (differentiated *v* poorly or undifferentiated) and MKI (low or intermediate *v* high) to evaluate tumor histology. For LDH, median value was used to dichotomize the cohort; LDH less than 580 U/L was classified as low, and 580 U/L or greater was classified as high.

Fisher's exact tests were performed for prognostic factors versus metastatic pattern. For event-free survival (EFS), time to event was calculated as time from enrollment to first occurrence of relapse, progressive disease, secondary malignancy, or death as a result of any cause or to time of last patient contact, if no event occurred. For overall survival (OS), time to event was time from enrollment until death or time of last contact, if alive. Survival was estimated using the Kaplan-Meier method,[22] and subgroups were compared by log-rank test. EFS and OS are expressed as the 5-year estimate plus or minus SE.[23]

A Cox model on EFS was used to explore the possibility of a better age cutoff to define stage 4S disease.[24] The subset of 717 patients with stage 4S metastatic pattern (ie, including some stage 4 patients > 1 year of age) was repeatedly divided into two age groups. *P* values and hazard ratios for older versus younger patients were calculated, whereby the optimal age cutoff was statistically significant and maximized the difference in EFS between older and younger patients (ie, largest hazard ratio). The selected age cutoff was used in other Cox models to test binary age in combination with one biologic factor at time, and another model was used to identify all factors independently predictive of EFS.

Survival tree regression was used to determine if biologic factors could improve risk groupings for patients younger than 18 months of age with metastases, either in addition to or in combination with age and metastatic pattern.[21,25,26] Proportional hazards assumption was confirmed by visual inspection of survival curves and plots of log(time) versus log[−log(S[time])].

RESULTS

EFS and OS by Age and Pattern of Metastases

In the overall cohort of patients age 0 to 18 months with metastases, 5-year EFS and OS (± SE) were 70% ± 2% and 75% ± 1%,

respectively (Table 1). Five-year EFS was significantly higher for patients with 4S pattern of metastases (77% ± 2%) compared with patients with stage 4 pattern of metastases (64% ± 2%; $P < .001$; Table 1; Fig 2A). Five-year EFS was also significantly higher for stage 4S pattern age younger than 12 months (79% ± 2%) than for stage 4 pattern age younger than 12 months (70% ± 2%; $P < .001$; Fig 2B). In contrast, EFS for toddlers age 12 to 18 months with stage 4S pattern (55% ± 8%) was not significantly different from EFS for toddlers with stage 4 pattern (50% ± 4%; $P = .39$; Fig 2C). EFS was also improved for younger patients age younger than 12 months compared with that for patients age 12 to 18 months, overall (Fig 2D), and within each metastatic pattern (Figs 2E, 2F). OS paralleled EFS in all cases.

Table 1. EFS and OS in Patients With Metastatic Neuroblastoma < 18 Months of Age (n = 1,675)

Characteristic	Patients No.	Patients %	5-Year EFS ± SE (%)	5-Year EFS P	5-Year OS ± SE (%)	5-Year OS P
All patients	1,675		70 ± 2		75 ± 1	
Pattern of metastatic disease				< .001		< .001
Stage 4S	717	43	77 ± 2		84 ± 2	
Stage 4	958	57	64 ± 2		69 ± 2	
Age, months				< .001		< .001
< 12	1,310	78	75 ± 2		82 ± 1	
12-18	365	22	51 ± 3		53 ± 3	
MYCN amplification				< .001		< .001
No	1,070	79	83 ± 2		90 ± 1	
Yes	282	21	28 ± 4		32 ± 4	
Unknown	323					
Ploidy				< .001		< .001
> 1 (hyperdiploid)	548	73	81 ± 3		87 ± 2	
≤ 1 (diploid, hypodiploid)	206	27	59 ± 6		63 ± 6	
Unknown	921					
Histology				< .001		< .001
Favorable	592	79	86 ± 2		92 ± 2	
Unfavorable	156	21	38 ± 6		39 ± 6	
Unknown	927					
MKI				< .001		< .001
Low, intermediate	513	84	84 ± 2		90 ± 2	
High	100	16	38 ± 7		38 ± 7	
Unknown	1,062					
11q				.0376		.55
Normal	145	80	77 ± 6		84 ± 5	
Aberration	36	20	54 ± 16		83 ± 13	
Unknown	1,494					
1p				< .001		< .001
Normal	284	73	83 ± 3		91 ± 3	
Aberration	105	27	43 ± 7		49 ± 7	
Unknown	1,286					
LDH, U/L				< .001		< .001
< 587	427	43	83 ± 2		91 ± 2	
≥ 587	555	57	60 ± 3		64 ± 3	
Unknown	693					
Initial treatment				< .001		< .001
Surgery and observation	254	21	86 ± 3		95 ± 2	
Chemotherapy and transplantation	967	79	64 ± 2		71 ± 2	
Unknown	454					
Primary tumor location				.0011		< .001
Nonadrenal primary	586	36	75 ± 2		81 ± 2	
Adrenal primary	1,022	64	67 ± 2		72 ± 2	
Unknown	67					
Grade of neuroblastoma differentiation				.79		.53
Differentiating	54	8	76 ± 6		83 ± 5	
Undifferentiated	590	92	75 ± 3		81 ± 3	
Unknown	1,031					

Abbreviations: EFS, event-free survival; LDH, lactic dehydrogenase; MKI, mitosis-karyorrhexis index; OS, overall survival.

Distribution of Clinical and Biologic Characteristics

To understand these differences in outcome, we assessed associations of age and pattern of metastases with poor prognostic features (Table 2). For patients with stage 4S pattern, the proportion of patients with unfavorable features was significantly higher among toddlers (age 12 to 18 months) than infants (age < 12 months) for *MYCN* amplification, 1p aberration, unfavorable histology, high MKI, and high LDH. However, the proportion with adrenal primary was higher for patients age younger than 12 months than for those age 12 to 18 months. In comparing infants versus toddlers within the subgroup with stage 4 pattern, a significantly higher proportion of patients age 12 to 18 months had unfavorable features: *MYCN* amplification, diploidy, unfavorable histology, and high MKI. In contrast to stage 4S pattern, in stage 4 pattern, more toddlers than infants had an adrenal primary.

In infants, unfavorable biologic prognostic features were also significantly more frequent in stage 4 than stage 4S pattern, including *MYCN* amplification, diploidy, 1p aberration, unfavorable histology, high MKI, and high LDH. Adrenal primary was observed in more infants with stage 4S pattern compared with stage 4 pattern. In contrast, the proportion of unfavorable prognostic features was not significantly different between toddlers with stage 4 and toddlers with 4S pattern, except for adrenal primary, which was more common in stage 4 pattern.

The following subgroups had a significantly higher proportion of patients who received initial treatment with chemotherapy or other intensive therapy: among infants, more stage 4 than 4S pattern; toddlers, more stage 4S than stage 4 pattern; within stage 4S pattern, more toddlers than infants.

EFS and OS by Prognostic Factors

In the cohort of patients age 0 to 18 months with metastatic disease, univariate analyses revealed that both EFS and OS were statistically significantly worse for toddlers and patients with stage 4 pattern, *MYCN* amplification, diploidy, unfavorable histology, high MKI, 1p LOH or aberration, high LDH, and adrenal primary (Table 1; Appendix Tables A1-A4, online only). EFS was worse for patients with 11q LOH or aberration ($P = .0376$), but OS was not ($P = .55$). Patients whose initial treatment plan included chemotherapy or more intensive therapy had lower EFS ($P < .001$) and OS ($P < .001$; Table 1). Grade of differentiation did not seem to affect prognosis in this cohort and was excluded from the other analyses.

Distribution of Outcome by Age

We next evaluated the prognostic impact of age within the cohort of patients with metastatic disease age 0 to 18 months. Five-year EFS for patients younger than age 19 days with metastatic disease was less than 71% for all subgroups; the subgroup with the lowest EFS was made up of those 7 to 18 days of age with stage 4 pattern (58% at 5 years; Appendix Fig A1, online only). The most favorable outcomes were in patients diagnosed at 19 to 38 days of age. Thereafter, EFS gradually decreased with increasing

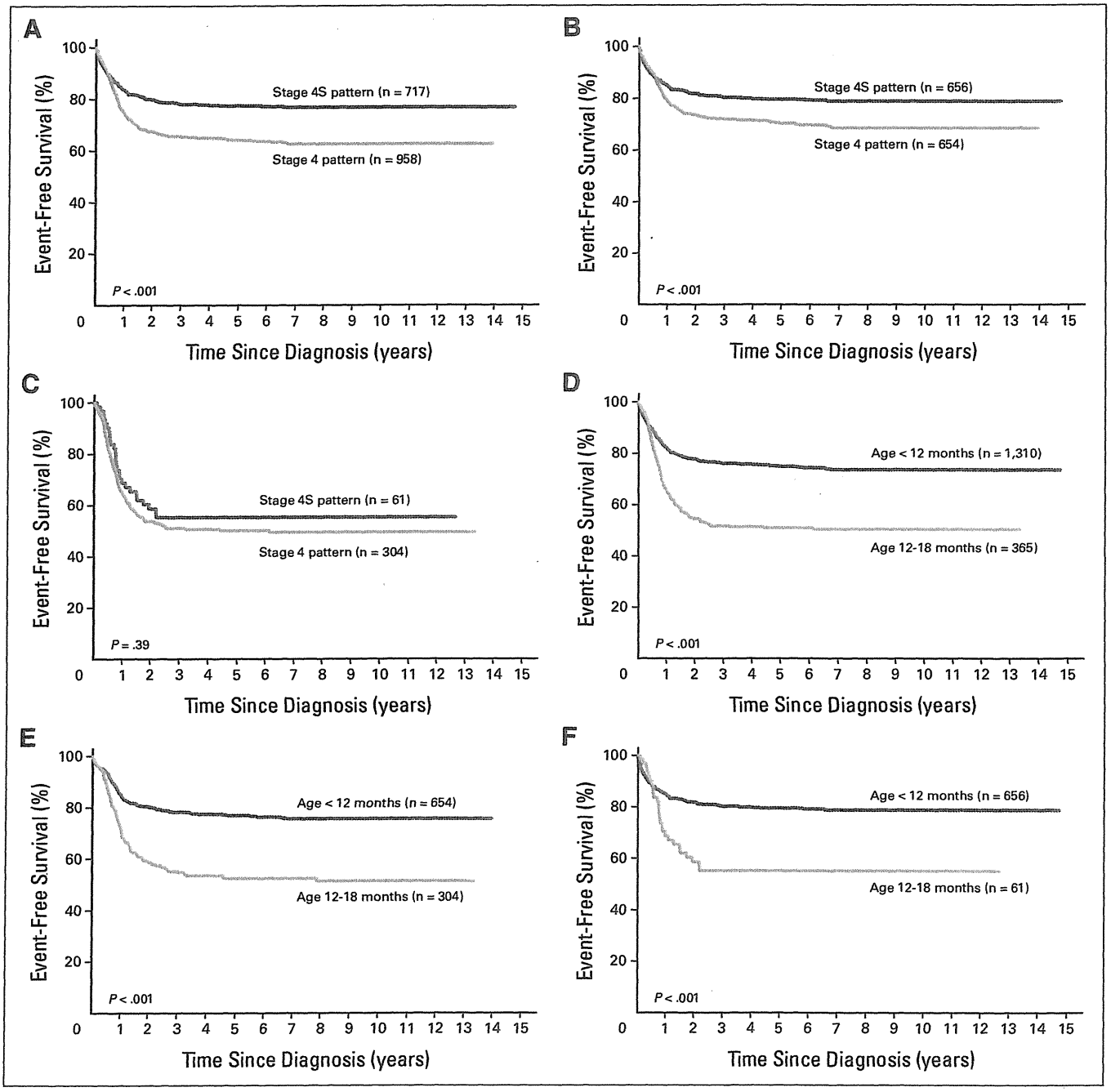

Fig 2. Event-free survival (EFS) comparisons by age and stage. EFS by stage for (A) all patients age 0 to 18 months with metastatic disease (n = 1,675), (B) infants age younger than 12 months (n = 1,310), and (C) toddlers age 12 to 18 months (n = 365). EFS by age for (D) all patients (n = 1,675), (E) patients with stage 4 pattern (n = 958), and (F) patients with stage 4S pattern (n = 717).

age in both 4 and 4S pattern, although EFS was lower for stage 4 pattern in almost every age group (Appendix Fig A1).

Within the cohort of patients with 4S pattern, we sought to determine whether the 365-day age cutoff maximized the outcome difference between younger and older patients. For patients with 4S pattern, those younger than 19 days of age had a 1.5 times greater risk of an event than patients 20 to 547 days of age, and those 365 days of age or older had a 2.31 times greater risk of an event than those who were younger than 365 days of age (Appendix Table A5, online only). No optimal age cutoff was identified, because the maximum hazard ratio was for the oldest group; risk for an event gradually increased with increasing age. Any choice of age cutoff greater than 226 days would be reasonable, so we made no change to the existing 365-day cutoff.

Multivariable Analysis

In univariate analyses, all factors were statistically significantly predictive of EFS except for grade of differentiation (Table 1). Significance of each factor was maintained when each was tested in combination with age in a multivariable Cox model (ie, testing to see if age and given factor were independently predictive of EFS; Table 3). In a

Table 2. Association of Risk Factors by Pattern of Metastases Within Age Subgroups and by Age Within Pattern of Metastases Subgroups

Unfavorable Tumor Feature	Total % of Patients* (n = 1,675)	Age (months)				Pattern of Metastases			
		< 12 (n = 1,310)		12 to 18 (n = 365)		Stage 4S (n = 717)		Stage 4 (n = 958)	
		4S v 4 Pattern (%)	P	4S v 4 Pattern (%)	P	Age < 12 v 12 to 18 Months (%)	P	Age < 12 v 12 to 18 Months (%)	P
MYCN amplified	21	8 v 20	**< .001**	39 v 48	NS	8 v 39	**< .001**	20 v 48	**< .001**
Diploidy	27	21 v 28	**.0323**	32 v 41	NS	21 v 32	NS	28 v 41	**.0178**
11q aberration	20	10 v 21	NS	38 v 34	NS	10 v 38	**.06**	21 v 34	NS
1p aberration	27	16 v 30	**.0036**	50 v 46	NS	16 v 50	**.0032**	30 v 46	NS
Unfavorable histology	21	7 v 23	**< .001**	52 v 48	NS	7 v 52	**< .001**	23 v 48	**< .001**
Grade: undifferentiated	92	93 v 90	NS	91 v 92	NS	93 v 91	NS	90 v 92	NS
High MKI	16	4 v 17	**< .001**	50 v 43	NS	4 v 50	**< .001**	17 v 43	**< .001**
High LDH	57	44 v 63	**< .001**	67 v 72	NS	44 v 67	**.0059**	63 v 72	NS
Adrenal primary	64	73 v 56	**< .001**	43 v 66	**.0008**	73 v 43	**< .001**	56 v 66	**.0032**
Initial treatment: chemotherapy or other intensive	79	58 v 93	**< .001**	100 v 92	**.0476**	58 v 100	**< .001**	93 v 92	NS

NOTE. Bold font indicates significance.
Abbreviations: LDH, lactate dehydrogenase; MKI, mitosis-karyorrhexis index; NS, not significant ($P > .05$).
*No. of unknown patients excluded when calculating percentages with given characteristic.

multivariable Cox model testing more than two variables, *MYCN*, 11q, MKI, ploidy, and LDH were independently predictive of EFS (Appendix Table A6, online only).

A survival tree regression model identified *MYCN* amplification as the most highly prognostic factor, more so than age or metastatic pattern (Fig 3). Among patients with *MYCN* amplified tumors, MKI and then metastatic pattern (in low/intermediate MKI patients) were the most statistically significant predictors of outcome. Among those with *MYCN* nonamplified tumors, 11q was the most highly significant predictor of outcome. Among patients with 11q aberration, histology was significant, and in patients with normal 11q, 1p was significant. Of the 18 patients age 12 to 18 months with 4S pattern and *MYCN* nonamplified, normal 11q tumors, 5-year EFS and OS were 87.4% ± 10.3% and 100.0%, justifying their inclusion as very low risk in the INRG.

DISCUSSION

In this study, we have demonstrated that overall outcome for patients with neuroblastoma and stage 4S pattern is superior to that for patients with stage 4 pattern, and outcome for older patients is in general worse than that for younger patients (with exception of patients < 19 days of age). Age and metastatic pattern are highly significant prognostic factors.[21,27] However, age serves as a surrogate for evolving tumor biology in growing children, so it is not surprising that tumor biology is shown here to be more important than metastatic pattern or age. In patients younger than 18 months old with metastases, *MYCN* gene amplification, 11q aberration, MKI, 1p aberration, histology, and metastatic pattern can be used to classify patients into subgroups that are statistically significantly different in terms of outcome. The reason that toddlers age 12 to 18 months have similar EFS regardless of metastatic pattern seems to be because of similar frequencies of unfavorable biologic features for stage 4 and 4S pattern in the toddler age group.

INSS stage 4S has been established as having superior outcome compared with historical results with INSS stage 4 disease in infants younger than 12 months of age.[3,4] However, *MYCN* gene amplification has been shown to be an extremely important prognostic factor in infants with metastatic neuroblastoma in multiple cooperative studies, for infants with both stage 4S[3,9] and stage 4 disease.[28-30] Infants with either stage 4 or 4s neuroblastoma and *MYCN* gene amplification have a 2-year EFS of less than 30% despite intensive therapy,[28,30] whereas those without *MYCN* amplification may have a 2-year survival of greater than 90% with minimal or no chemotherapy.[29,31] Because of the rarity of *MYCN* amplification in infants with 4S neuroblastoma (0% to 10%), it has been difficult to show without the help

Table 3. Bivariate Analysis of Risk Factors in Stage 4S Metastatic Pattern

Risk Factor (category of increased risk)	Sample Size	Hazard Ratio	95% CI	P
Age (12 to < 18 months)	717	2.3	1.5 to 3.5	< .001
Age	564	NS		.33
MYCN (amplified)		4.1	2.6 to 6.2	< .001
Age	85	NS		.30
11q (aberration)		5.0	1.6 to 15.7	.0052
Age	196	NS		.68
1p (LOH)		3.3	1.7 to 6.6	< .001
Age	305	2.8	1.3 to 6.5	.0127
Ploidy (diploid)		1.9	1.0 to 3.8	.05
Age	337	NS		.87
Histologic classification (unfavorable)		4.3	2.2 to 8.4	< .001
Age	296	2.4	1.2 to 5.0	.0139
Grade (differentiated)		NS		.77
Age	282	NS		.67
MKI (high)		2.9	1.2 to 7.1	.0183
Age	460	2.1	1.3 to 3.6	.0040
LDH (≥ 580 U/L)		2.4	1.6 to 3.6	< .001
Age	677	2.3	1.5 to 3.5	< .001
Adrenal primary site (Yes)		NS		.59
Age	545	2.1	1.3 to 3.3	.0029
Initial treatment (chemotherapy and intensive therapy)		1.7	1.1 to 2.6	.0161

Abbreviations: LDH, lactate dehydrogenase; LOH, loss of heterozygosity; MKI, mitosis-karyorrhexis index; NS, not shown because not statistically significant.

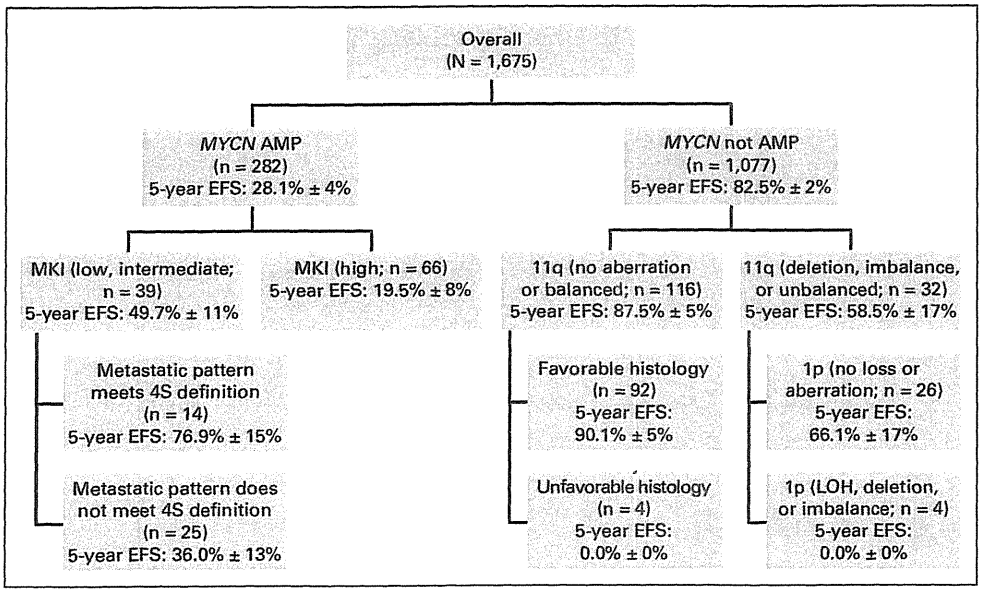

Fig 3. Survival tree regression analysis of patients with neuroblastoma younger than 18 months of age with metastatic disease (n = 1,675; event-free survival [EFS] ± SE). AMP, amplified; LOH, loss of heterozygosity; MKI, mitosis-karyorrhexis index.

of a large series such as the INRG database that *MYCN* status is prognostic independent of age and other factors. The favorable outcome for patients with stage 4 pattern without *MYCN* amplification was also extended to toddlers age 12 to 18 months. Two cooperative group analyses showed that this subgroup had a significantly superior survival to older patients with stage 4 disease as well as to those of the same age with *MYCN* gene amplification.[15,16] These findings prompted the revised INRG age limit for 4S metastatic pattern now designated Ms.[17]

In addition to *MYCN*, the other independently prognostic factors were 11q, MKI, ploidy, and LDH, despite the fact that a number of patients lacked information on these biologic variables. Within particular subsets in the survival tree, metastatic pattern, histology, and 1p were also significant. Attiyeh et al[32] reported 11q and 1p aberrations as independent unfavorable risk factors in a study of 915 patients, regardless of clinical risk classification. This study included nine of 50 patients with stage 4S and 11q aberration, although this small group was not analyzed separately. Spitz et al[33] compared 11q aberration in localized and 4S disease and found metastatic relapse rates to be 30% when 11q aberration was present and 3% with normal 11q status. Although a relatively low proportion of patients in our INRG series had assessment of 11q aberration (181 of 1,675 patients age < 18 months with metastases), the effect of 11q was so strong that even in this small sample, we found significance in multivariable analysis. Patients younger than 12 months or 12 to 18 months of age with *MYCN* amplified or 11q LOH tumors would not be considered low-risk patients and would warrant more intensive therapy despite the 4S pattern. Excluding such patients, there were only 18 patients who were age 12 to 18 months with *MYCN* not amplified and normal 11q tumors, with 5-year EFS and OS of 87.4 ± 10.3% and 100.0%, respectively.

Previous analyses of 4S disease have found unfavorable histology to be associated with decreased survival.[4,9] Diploid tumors have also been associated with poorer outcomes, but the prognostic benefits of hyperdiploid tumors seem to be limited to infants and toddlers age 12 to 18 months without *MYCN* amplification.[15] Elevated serum LDH may indicate increased tumor burden and has been identified as an independent poor prognostic factor.[3,9]

In our evaluation of infants with stage 4S disease, we found that risk of an event was high for patients of very young age, that the age subgroup with the best outcome was approximately 19 to 38 days, and that risk of an event increased gradually after age 38 days. Although the definition of young age varies by study, multiple groups have reported that infants younger than 2 to 3 months old have poorer OS than older infants.[3,4,9] Massive hepatomegaly in these infants can lead to respiratory, renal, and gastrointestinal impairment as well as coagulation abnormalities.[3] In the analysis by Nickerson et al[4] of 80 infants with 4S disease, five of the six recorded deaths occurred in infants younger than 2 months of age who had rapidly progressive abdominal disease. A literature review of 119 4S cases found that in 33 deaths, 11 of 12 deaths resulting from hepatomegaly occurred in infants diagnosed in the first 4 weeks of life.[13] These young infants with liver enlargement often are treated early and are at greater risk of death, thus explaining the observation in our INRG study that initial treatment is an unfavorable prognostic factor, as noted by others.[3]

Although this analysis used the largest cohort of patients with 4S metastatic pattern younger than 18 months of age, missing data and the rarity of some of the biologic tumor features resulted in some limitations. For example, some of the contributing groups at certain times allowed patients with so-called 4S disease younger than 12 months with tumors that crossed the midline as well as bone marrow involvement of more than 10%, characteristics that would have excluded patients from 4S categorization by the INSS definition; less than 10% bone marrow involvement was not required for any patient in the 12- to 18-month-old group with 4S pattern, because these patients were not defined as INSS 4S. It is unknown whether the size and stage of primary tumor are important in assigning 4S designation, but our study has shown that the pattern of metastases is less critical for risk group definitions than biologic variables. The most recent European infant protocols have used the metastatic pattern excluding macroscopic bone metastases but ignoring the primary tumor size as criteria for minimizing therapy in infants with metastatic neuroblastoma.[29] Finally, a variety of different treatment regimens were used, and thus, we were unable to adjust for treatment effect on EFS and OS. Acquisition of more complete data on biologic tumor features will be

critical for future clinical trials to provide improved assignment of treatment intensity and greater insight into the role of biologic and clinical tumor features on patient survival.

In conclusion, although the INSS stage 4S metastatic pattern has a more favorable outcome than stage 4 pattern in the age group of 0 to 18 months, biologic categorization of risk, particularly by *MYCN*, MKI, 11q, 1p, and histology, is more critical than metastatic pattern to assign risk-adapted therapy. In addition, infants in the very young age group (ie, age younger than 19 days) may require different management.

AUTHORS' DISCLOSURES OF POTENTIAL CONFLICTS OF INTEREST

The author(s) indicated no potential conflicts of interest.

AUTHOR CONTRIBUTIONS

Conception and design: Denah R. Taggart, Wendy B. London, Mary Lou Schmidt, Katherine K. Matthay
Financial support: Wendy B. London
Provision of study materials or patients: Tom F. Monclair, Akira Nakagawara, Bruno De Bernardi, Susan L. Cohn, Katherine K. Matthay
Collection and assembly of data: Wendy B. London, Tom F. Monclair, Akira Nakagawara, Bruno De Bernardi, Peter F. Ambros, Andrew D.J. Pearson, Susan L. Cohn, Katherine K. Matthay
Data analysis and interpretation: Denah R. Taggart, Wendy B. London, Mary Lou Schmidt, Steven G. DuBois, Peter F. Ambros, Susan L. Cohn, Katherine K. Matthay
Manuscript writing: All authors
Final approval of manuscript: All authors

REFERENCES

1. D'Angio G, Evans A, Koop C: Special pattern of widespread neuroblastoma with a favourable prognosis. Lancet 1:1046-1049, 1971
2. Brodeur GM, Pritchard J, Berthold F, et al: Revisions of the international criteria for neuroblastoma diagnosis, staging, and response to treatment. J Clin Oncol 11:1466-1477, 1993
3. Schleiermacher G, Rubie H, Hartmann O, et al: Treatment of stage 4s neuroblastoma: Report of 10 years' experience of the French Society of Paediatric Oncology (SFOP). Br J Cancer 89:470-476, 2003
4. Nickerson HJ, Matthay KK, Seeger RC, et al: Favorable biology and outcome of stage IV-S neuroblastoma with supportive care or minimal therapy: A Children's Cancer Group study. J Clin Oncol 18:477-486, 2000
5. Bourhis J, Dominici C, McDowell H, et al: N-myc genomic content and DNA ploidy in stage IVS neuroblastoma. J Clin Oncol 9:1371-1375, 1991
6. DuBois SG, Kalika Y, Lukens JN, et al: Metastatic sites in stage IV and IVS neuroblastoma correlate with age, tumor biology, and survival. J Pediatr Hematol Oncol 21:181-189, 1999
7. Hachitanda Y, Hata J: Stage IVS neuroblastoma: A clinical, histological, and biological analysis of 45 cases. Hum Pathol 27:1135-1138, 1996
8. Wang Q, Diskin S, Rappaport E, et al: Integrative genomics identifies distinct molecular classes of neuroblastoma and shows that multiple genes are targeted by regional alterations in DNA copy number. Cancer Res 66:6050-6062, 2006
9. Katzenstein HM, Bowman LC, Brodeur GM, et al: Prognostic significance of age, MYCN oncogene amplification, tumor cell ploidy, and histology in 110 infants with stage D S neuroblastoma: The pediatric oncology group experience—A pediatric oncology group study. J Clin Oncol 16:2007-2017, 1998
10. Guo C, White PS, Weiss MJ, et al: Allelic deletion at 11q23 is common in MYCN single copy neuroblastomas. Oncogene 18:4948-4957, 1999
11. Maris JM, Hogarty MD, Bagatell R, et al: Neuroblastoma. Lancet 369:2106-2120, 2007
12. Maris JM, Matthay KK: Molecular biology of neuroblastoma. J Clin Oncol 17:2264-2279, 1999
13. van Noesel MM, Heahlen K, Hakvoort-Cammel FG, et al: Neuroblastoma 4S: A heterogeneous disease with variable risk factors and treatment strategies. Cancer 80:834-843, 1997
14. Schneiderman J, London WB, Brodeur GM, et al: Clinical significance of MYCN amplification and ploidy in favorable-stage neuroblastoma: A report from the Children's Oncology Group. J Clin Oncol 26:913-918, 2008
15. George RE, London WB, Cohn SL, et al: Hyperdiploidy plus nonamplified MYCN confers a favorable prognosis in children 12 to 18 months old with disseminated neuroblastoma: A Pediatric Oncology Group study. J Clin Oncol 23:6466-6473, 2005
16. Schmidt ML, Lal A, Seeger RC, et al: Favorable prognosis for patients 12 to 18 months of age with stage 4 nonamplified MYCN neuroblastoma: A Children's Cancer Group Study. J Clin Oncol 23: 6474-6480, 2005
17. Monclair T, Brodeur GM, Ambros PF, et al: The International Neuroblastoma Risk Group (INRG) staging system: An INRG Task Force report. J Clin Oncol 27:298-303, 2009
18. Shimada H, Ambros IM, Dehner LP, et al: The International Neuroblastoma Pathology Classification (the Shimada system). Cancer 86:364-372, 1999
19. Bagatell R, Beck-Popovic M, London WB, et al: Significance of MYCN amplification in international neuroblastoma staging system stage 1 and 2 neuroblastoma: A report from the International Neuroblastoma Risk Group database. J Clin Oncol 27: 365-370, 2009
20. Ambros PF, Ambros IM, Brodeur GM, et al: International consensus for neuroblastoma molecular diagnostics: Report from the International Neuroblastoma Risk Group (INRG) Biology Committee. Br J Cancer 100:1471-1482, 2009
21. Cohn SL, Pearson AD, London WB, et al: The International Neuroblastoma Risk Group (INRG) classification system: An INRG Task Force report. J Clin Oncol 27:289-297, 2009
22. Kaplan EL, Meier P: Nonparametric estimation from incomplete observations. J Am Stat Assoc 53:457-481, 1958
23. Peto R, Pike MC, Armitage P, et al: Design and analysis of randomized clinical trials requiring prolonged observation of each patient: I. Introduction and design. Br J Cancer 34:585-612, 1976
24. Cox DR: Regression models and life tables. J R Stat Soc B 34:187-220, 1972
25. Segal MR: Extending the elements of tree-structured regression. Stat Methods Med Res 4: 219-236, 1995
26. Segal MR, Bloch DA: A comparison of estimated proportional hazards models and regression trees. Stat Med 8:539-550, 1989
27. London WB, Castleberry RP, Matthay KK, et al: Evidence for an age cutoff greater than 365 days for neuroblastoma risk group stratification in the Children's Oncology Group. J Clin Oncol 23:6459-6465, 2005
28. Schmidt ML, Lukens JN, Seeger RC, et al: Biologic factors determine prognosis in infants with stage IV neuroblastoma: A prospective Children's Cancer Group study. J Clin Oncol 18:1260-1268, 2000
29. De Bernardi B, Gerrard M, Boni L, et al: Excellent outcome with reduced treatment for infants with disseminated neuroblastoma without *MYCN* gene amplification. J Clin Oncol 27:1034-1040, 2009
30. Canete A, Gerrard M, Rubie H, et al: Poor survival for infants with *MYCN*-amplified metastatic neuroblastoma despite intensified treatment: The International Society of Paediatric Oncology European neuroblastoma experience. J Clin Oncol 27: 1014-1019, 2009
31. Baker DL, Schmidt ML, Cohn SL, et al: Outcome after reduced chemotherapy for intermediate-risk neuroblastoma. N Engl J Med 363:1313-1323, 2010
32. Attiyeh EF, London WB, Mosse YP, et al: Chromosome 1p and 11q deletions and outcome in neuroblastoma. N Engl J Med 353:2243-2253, 2005
33. Spitz R, Hero B, Simon T, et al: Loss in chromosome 11q identifies tumors with increased risk for metastatic relapses in localized and 4S neuroblastoma. Clin Cancer Res 12:3368-3373, 2006

